



Universidade Federal do Rio Grande do Sul
Instituto de Física
Programa de Pós-Graduação em Física

Generalized Mean-Field Approximations for Evolutionary Games on Lattices
(Aproximações Generalizadas de Campo Médio para Jogos Evolutivos em Redes)

Guilherme Marasca Wiener

Brazil, 2021

Guilherme Marasca Wiener

Generalized Mean-Field Approximations for Evolutionary Games on Lattices

(Aproximações Generalizadas de Campo Médio para Jogos Evolutivos em Redes)

Dissertação de Mestrado apresentada ao Programa de Pós-Graduação em Física da UFRGS, como parte dos requisitos necessários para a obtenção do Título de Mestre em Física.

Universidade Federal do Rio Grande do Sul – UFRGS

Instituto de Física

Programa de Pós-Graduação em Física

Supervisor: Mendeli Henning Vainstein

Brazil

2021

CIP - Catalogação na Publicação

Wiener, Guilherme Marasca
Generalized Mean-Field Approximations for
Evolutionary Games on Lattices / Guilherme Marasca
Wiener. -- 2021.
86 p f.
Orientador: Mendeli Henning Vainstein.

Dissertação (Mestrado) -- Universidade Federal do
Rio Grande do Sul, Instituto de Física, Programa de
Pós-Graduação em Física, Porto Alegre, BR-RS, 2021.

1. Extended Mean-Field Approximations. 2.
Evolutionary Game Theory. 3. Local Structure Theory.
4. Prisoner's Dilemma. 5. Diluted Lattices. I.
Vainstein, Mendeli Henning, orient. II. Título.

Agradecimentos

Agradeço especialmente à Alice e à Luciana, que sem toda ajuda de vocês no período mais difícil este trabalho não teria sido completado.

Agradeço todos os amigos que me acompanharam e me ajudaram muito no decorrer destes anos. Alan, Bruna, Carol, Guiga e Matheus são nomes que destaco com carinho especial. Agradeço aos colegas de curso e da sala M201 pelos momentos compartilhados.

Agradeço aos enfermeiros, psiquiatras e os outros internados do IPQ de Santa Catarina que me ajudaram a repensar na vida.

Agradeço ao meu pai e à minha mãe, pelo apoio incondicional.

Agradeço ao Mendeli por suas orientações, elucidações e ideias que permeiam este trabalho.

Agradeço a todos que participaram do Grupo de Teoria de Jogos do IF pelas suas apresentações e discussões.

Agradeço pelo apoio financeiro do Conselho Nacional de Desenvolvimento Científico e Tecnológico (CNPq), sem o qual este trabalho nunca teria sido realizado. Agradeço ao Instituto de Física e a UFRGS pelo espaço e oportunidade.

Abstract

Evolutionary game theory offers interesting models for the study of the emergence and maintenance of cooperation. One mechanism that can maintain cooperation in a Prisoner's Dilemma is affixing players in a network, under imitation dynamics (NOWAK; MAY, 1992). Interestingly, it was found that dilution of this lattice may lead to an enhancement of cooperation (VAINSTEIN; ARENZON, 2001), and this increase has a connection to the percolation threshold of the lattice (WANG; SZOLNOKI; PERC, 2012a). We intend to explore this phenomenon using extended mean-field approximations. We didactically present the construction of these approximations and develop a simple and clear algorithm that systematically implements an approximation method based on the ideas presented by Gutowitz & Victor (1987), explaining them in a simple way of under/overrepresentation of structures. We use this method to explore and compare different approximations for the square lattice. We found that the most commonly used pair approximation for the square lattice does not have the best predictions amongst the pair approximations, at least in the evolutionary game system analysed. We use pair approximations for different diluted lattices to explore the connection of percolation and the increase of cooperation. The pair approximations reproduce the phenomenon in a qualitative way. We find that, for the pair approximation, the site-occupancy at which the peak of cooperation disappears can be changed by alterations in the noise of the imitation function probability, including changing the peak to beyond the percolation threshold. These could be explained if the increase of cooperation happens due to favorable local configurations becoming more probable around some site occupation values, which could be confused with the percolation threshold.

Keywords: Evolutionary Game Theory. Prisoner's Dilemma. Extended Mean-Field Approximations. Local Structure Theory. Percolation Threshold. Games on Diluted Lattices.

Resumo

A Teoria de Jogos Evolutivos oferece modelos interessantes para o estudo da emergência e manutenção da cooperação. Um mecanismo que consegue manter a cooperação no Dilema do Prisioneiro é a fixação dos jogadores em uma rede, usando dinâmica de imitação (NOWAK; MAY, 1992). Um resultado interessante que foi encontrado é que a diluição dessas redes pode levar a um aumento da cooperação (VAINSTEIN; ARENZON, 2001), e este aumento tem uma conexão com o limite de percolação crítico da rede (WANG; SZOLNOKI; PERC, 2012a). Nós pretendemos explorar esse fenômeno usando aproximações de campo-médio extendidas. Como parte dessa exploração, apresentamos didaticamente a construção dessas aproximações e desenvolvemos um algoritmo claro e simples para sistematicamente implementar um método de aproximação baseado nas idéias apresentadas por Gutowitz & Victor (1987), explicando-as de uma forma simples, através do conceito de sub/super-representação de estruturas. Com o uso deste método para explorar e comparar diferentes aproximações na rede quadrada, encontramos que a aproximação mais comumente usada não apresenta as melhores previsões entre as diferentes aproximações de pares para a rede quadrada, ao menos no sistema de jogo evolucionário analisado. Usando aproximações de pares para diferentes redes diluídas, exploramos a conexão entre percolação e o aumento de cooperadores. As aproximações de pares reproduzem o fenômeno de uma forma qualitativa. Descobrimos que, ao menos para as aproximações de pares, o pico de cooperação desaparece em diferentes ocupações de rede com alterações do ruído na função da probabilidade de imitação, incluindo mudanças para além do limite crítico de percolação. Esses fatos podem ser explicados caso o aumento da cooperação esteja ligada a configurações locais mais favoráveis se tornarem mais provável para alguns valores de ocupação da rede, valores estes que poderiam ser confundidos com o valor crítico para a percolação.

Palavras-chave: Teoria de Jogos Evolutivos, Dilema do Prisioneiro, Aproximações de campo-médio extendidas, Limite crítico de percolação, Jogos em Redes Diluídas.

Contents

1	INTRODUCTION	1
2	THE APPROXIMATE ANALYTICAL SOLUTION	7
2.1	A First Step: the Mean-field Approach	8
2.2	Local pair correlations approach	10
2.3	Local Structure Theory	15
2.3.1	Definitions: Frame, Frame Format, Block	16
2.3.2	Closure condition and probability for smaller blocks	18
2.3.3	Approximation of the probability of larger blocks in one dimension	19
2.4	Automated Extension Algorithm	20
2.4.1	Problem with cyclic structures: Losing normalization and closure	22
2.5	Code Implementation and Example of Application	23
2.5.1	Step 1: Finding all squares in the extended frame	24
2.5.2	Step 2 for R=1: Removing one site	26
2.5.3	Step 2 for R=2: Removing two sites	26
2.5.4	Step 2 for R=3: Removing three sites	27
2.5.5	Step 3: Writing the approximation for the extended frame	28
2.6	Reducing Computational Costs	28
2.6.1	Symmetries	29
2.6.2	Inactive states	30
2.7	Experimenting with different Extended Frames and Comparing Ap- proximations	30
2.7.1	Comparing Pair Approximations	33
2.7.2	Comparing Square Approximations	35
2.7.3	Comparing Cross Approximations	37
2.7.4	Guiding Principles for choosing the extended frame	38
3	APPLICATIONS TO DILUTED LATTICES	41
3.1	Approximations for the Diluted Lattice	42
3.2	Results for the Diluted Square Lattice	44
3.2.1	Possible explanation for the diluted square lattice	47
3.3	Prisoner's Dilemma in other lattices	50
4	DISCUSSION	53
	BIBLIOGRAPHY	55

Appendices	59
APPENDIX A – IS THE WEAK PD WITH SELF-INTERACTION A SNOWDRIFT GAME?	61
APPENDIX B – APPROXIMATIONS FOR THE SQUARE LAT- TICE	63
B.1 Pair approximations	67
B.2 Square approximations	67
B.3 Cross Approximations	68
APPENDIX C – PAIR APPROXIMATIONS FOR DIVERSE LAT- TICES	69
C.1 Pair Approximation for the N Bethe trees	69
C.2 Pair Approximation for the Honeycomb Lattice	69
C.3 Pair Approximation for the Cubic Lattice	70
C.4 Pair Approximation for the Triangular Lattice	71
APPENDIX D – TRANSITION FUNCTION ω	73

1 Introduction

We will start with a brief overview of the history of Game Theory (GT), introducing some of the important concepts and results of this area. We will be presenting the context in which the mathematical models were created, as a way to justify the choices made in this dissertation.

Without further ado, we begin by defining what a *game* is in *Game Theory*, as the word can cause some confusion to the unfamiliarized reader. We selected two of the four definitions for game in the [Merriam-Webster Online Dictionary \(2021\)](#):

1. activity engaged in for diversion or amusement;
2. a physical or mental competition conducted according to rules with the participants in direct opposition to each other.
3. a procedure or strategy for gaining an end

While the first definition may be more used in the daily life, the second captures the meaning of a non-cooperative game in GT more closely, and the third can even capture the class of cooperative games in GT. A chess match, bargaining with a vendor to lower the price of an item, or fighting an animal so one does not become food can all be considered a game by these definitions (and some, or even all, of such activities may not be considered *fun*).

Game Theory is said to start as a formal field with the works of [Von Neumann & Morgenstern \(1944\)](#) on cooperative games, where a group of players find the best solution and can be bound to it, through some sort of central control or contract. It is followed by an increase in scope with the study of non-cooperative games, where binding contracts are not always available¹. The focus passes to which strategy may earn the best payoff for an individual player. Generally, it is considered that players are perfectly rational, and that this is common knowledge to them. A perfectly rational player is the one that chooses the best strategy, with highest payoff for himself. Defining what is the best strategy is not simple in many situations, and that is a central problem in GT ([SZABO; FATH, 2007](#), p. 99).

One attempt of defining what the best strategies are is through the concept of *Nash equilibrium*. The strategy of a group of players is considered to be at a Nash equilibrium if any player individually changing their strategy would lead to a decrease in their payoff ([NASH, 1950](#)). We could assume a perfectly rational player would play a strategy in the set of the Nash equilibrium. This seems reasonable, but, in many games, such as the Tragedy

¹ Contracts can be considered as a part of the game itself, making cooperative games a subset of non-cooperative games.

of the Commons and the Prisoner's Dilemma, the Nash equilibrium strategies lead to a worse individual payoff for all players when compared with other set of strategies.

In a game of Prisoners' Dilemma (PD), the two players simultaneously choose between two possible actions: Cooperate or Defect. Depending on the action of both players, each gains a payoff. If both cooperate, they both receive R (the Reward). If both defect, they both receive P (the Punishment). If player X defects while player Y cooperates, player X receives T (the Temptation), while player Y receives S (the Sucker's payoff), and vice-versa. These payoffs can be visualized in a matrix form for easier comprehension in Table 1a. The dilemma happens when conditions $T > R > P > S$ and $2R > T + S$ are met², as the Nash equilibrium set of strategies is both players defecting, each receiving the P payoff, which is smaller than R if both cooperated.

		Player Y	
		C	D
Player X	C	R	S
	D	T	P

(a) Payoff in the Prisoner's Dilemma game ($T > R > P > S$ and $2R > S + T$).

		Player Y	
		C	D
Player X	C	1	0
	D	b	0

(b) Payoff in the weak Prisoner's Dilemma game ($1 < b < 2$).

Table 1 – Tables presenting the PD and weak PD payoff for Player X and Player Y choosing to either cooperate (C) or defect (D). The weak PD game breaks the condition $P > S$ present in the PD game (payoff for defecting against a defector is larger than cooperating against it), because $P = S$ (and both equal to 0 in this parametrization).

The dilemma happens due to the following consideration: if your opponent cooperates, the action which leads to the highest payoff would be defecting, as you would receive T which is bigger than R ; if your opponent defects, the best action would be to defect too, as you would receive P which is bigger than S . The basis of the dilemma lies in that a mutual agreement to cooperate would yield a better payoff for both players but with no reliable way to assure cooperation, the *rational* choice leads both players choosing to defect. For details of the history, examples and more considerations about the Prisoner's Dilemma, we suggest the book by Poundstone (1993).

The Prisoner's Dilemma has been used to model the nuclear arms race between the United States and the Soviet Union during the Cold War. After acquiring the technology related to building nuclear weapons, actually building a vast, deployable atomic arsenal

² The condition $2R > T + S$ is necessary, as the players could agree to redistribute the payoff, gaining equal values, $(T + S)/2$, greater than if they both chose to cooperate, R . In the case of multiple rounds, alternating between cooperation and defection, in an out of sync way, the players could achieve this redistribution of payoff, and the best aggregated payoff would be this anti-coordination solution rather than cooperation. This condition imposes one of the fundamental characteristics of this dilemma: the greater aggregated payoff happens when both cooperate.

is costly, and if the country does not use the arsenal (as atomic bombs have not been military used since the second world war) it means a cost without a return. But if one country produced a nuclear arsenal and the other did not, the first one could use the military advantage as a potential threat in negotiations, so this potential advantage can be compared to the Temptation in the PD game and being at the other end of the stick of the threat can be considered the Sucker's payoff. If both countries produced they would incur an expensive cost, but neither would gain an advantage as making a nuclear attack without destroying all of the targets nuclear weapons would lead to retaliation, making a first attack actually a suicidal one (a state known as Mutual Assured Destruction). The cooperation in this case is the pacifist one, where both agree to not build an atomic arsenal. But, without ways to guarantee such deal, what we see in history is both countries producing massive stockpiles of atomic weapons, both players locked in a defecting position ([POUNDSTONE, 1993](#)).

We could have multiple, successive (finite) rounds of a PD game. In each round there is a choice between cooperating and defecting. The players can react to each other's actions. Because of that, when the players have memory, the strategies are more complex. Even then, mutual defection in all rounds is the only subgame perfect Nash equilibrium (a generalization of the Nash equilibrium to repeated, multiple round games) ([SZABO; FATH, 2007](#), p. 100). This is due to a backwards induction reasoning: in the last round, since there could be no retaliation against defecting, the best action is to defect. Since this is common knowledge to both, both will defect in the last turn. In the previous to last round, the best action is to defect, since you know in the last round both will be defecting, so no retaliation is possible. Following this inductive reasoning, extending to all rounds, defecting from start to finish becomes the Nash equilibrium.

An interesting result is obtained in the famous Axelrod's tournaments, where several strategies submitted by multiple people were played against each other in a multi-round PD and the strategy that had a better overall performance was the Tit-for-Tat (TFT) ([AXELROD, 1984](#)). TFT initiates with cooperation and after that, it just copies the action performed by the other player in the last round. This simple strategy, with a memory of only the previous round, can retaliate against non-cooperators and can establish and maintain mutual cooperation with cooperative players ([AXELROD; HAMILTON, 1981](#)). As pointed by [Axelrod \(1984, p. 20\)](#): "These results from the tournaments demonstrate that under suitable conditions, cooperation can indeed emerge in a world of egoists without central authority." The exploration of these suitable conditions for cooperation to arise and be maintained is fundamental to a comprehension of animal behaviour, and the PD provides an interesting mathematical framework for this.

The book by [Maynard \(1982\)](#) explores Evolutionary Game Theory (eGT), "where the concept of human rationality is replaced by that of evolutionary stability". A cen-

tral concept developed is that of an Evolutionary Stable Strategy, a strategy that, when adopted by the entire population, is resistant to invasion by a small number of mutants. According to [Maynard \(1982, p. 203\)](#), the TFT is an evolutionary stable strategy, and resistant to invasion from a strategy of always defecting for example (given the expected number of rounds to be high, in this case, the number of rounds is random and not known to players).

Countless criticisms to the classic GT assumptions of perfect rationality to model human behaviour can be given and is a fascinating subject of study, with many open issues and points of discussion. Arguments can be given in favour of the eGT analysis: generally the natural way of change is not by rational induction, but by Darwinian selection. Therefore, it is important to explore the evolution of strategies and adaptations to the environment as not static. In nature, genetically encoded strategies are slow to change, depending on the life span of generations for different reproductive rates and mutation rates to explore new strategies. In animal (human not excluded) behaviour, it is common to see learning by observation and trial and error rather than inductive reasoning ([SZABO; FATH, 2007, p. 101](#)). For this reason, a fundamental mechanism in eGT is that change in behaviour is based on copying strategies which are more successful (either through reproduction or observation learning) rather than reasoning.

Evolutionary Game Theory has found multiple different mechanisms that help sustain cooperation: kin selection; direct reciprocity; indirect reciprocity; group selection; and the one most interesting to our work, network reciprocity ([NOWAK, 2006](#)). As it was shown by [Nowak & May \(1992\)](#), even the simplest altruistic strategies, such as always cooperate, can survive playing a weak PD (payoff matrix defined in [Table 1b](#)) when players are fixed on a lattice and play against their neighbours, under deterministic rules of copying the neighbour's strategy with best performance. As indicated in the article, the important mark that allows for simple cooperators to survive defectors is the formation of clusters/groups of cooperator which can self protect against the effects of defection. This mechanism, fixating players in a lattice, has presented robust results favoring cooperators even under other deterministic and stochastic rules ([SZABO; FATH, 2007](#)).

One way to see the relevance of this mechanism is by comparing this interaction limited on a lattice with the geographic/movement limitation of animals in nature. The population is generally not well-mixed and organisms (or its descendants) tend to face each other multiple times due to geographical constriction. Some studies have been done about different underlying structures, from different lattices ([SZABO; VUKOV; SZOLNOKI, 2005](#)) to scale-free (real) networks ([WU et al., 2007; SZOLNOKI; PERC; DANKU, 2008](#)), and show that the persistence of cooperation exists. Besides that, it has also been questioned whether the introduction of mobility would break the benefits given by this network limitation with different answers for different cases ([VAINSTEIN; T.C. SILVA;](#)

[ARENZON, 2007](#); [SICARDI et al., 2009](#); [MELONI et al., 2009](#)).

We are interested particularly in the case of a not fully occupied regular network, some sites being randomly left empty. In [Vainstein & Arenzon \(2001\)](#), it is seen that for some cases, the removal of some players from a square lattice can lead to a rise of cooperation in the steady state. This could be related to the problem of overpopulation/occupation already known in experiments with rats ([CALHOUN, 1962](#)) and even discussed in very early population models ([MALTHUS, 1878](#)). On the other hand, it could be related to what is seen in other networks that heterogeneity in the degree distribution may boost cooperation ([PERC; SZOLNOKI, 2008](#)). In [Wang, Szolnoki & Perc \(2012a\)](#) and [Wang, Szolnoki & Perc \(2012b\)](#), it is seen that, for the square, triangular, honeycomb and cubic lattices this cooperation increase occurs near the critical percolation threshold for the specific lattice. As is known from graph theory, this threshold is connected to the existence of a infinite connected group and a regime change in how far information can travel in this diluted lattice ([ESSAM, 1980](#); [GRIMMETT et al., 1999](#)).

We will investigate the problem of game theory in diluted lattices in [Chapter 3](#) using extended mean-field approximations, while in [Chapter 2](#) we discuss how to construct these extended mean-field approximations for lattices, exploring different constructions for the undiluted square lattice.

2 The Approximate Analytical Solution

Sometimes, we have no way to analytically solve a lattice game model without making approximations based on assumptions about the system. We intend to create a simple and clear algorithm that systematically implements an approximation method for different lattices and game models, making it easier to computationally explore multiple variations of lattices or game models.

We will start by introducing simple cases of this method to establish some notation to later formalize it. We start in section 2.1 by introducing the mean-field approach, which assumes that the correlation between players on the lattice can be ignored, applying it to players fixated on a square lattice playing the weak PD with their four neighbours, and the copying mechanism is defined by a function ω of the difference of payoff between the pair randomly chosen for comparison. This method fails to predict an essential feature present in Monte Carlo (MC) simulations for the system: the coexistence of strategies. In section 2.2, we will then introduce an improved method that considers neighbour-to-neighbour (pair) correlations. Applying the pair method to the same system, we show that it predicts coexistence of strategies.

We present the Local Structure Theory method for building approximations, in section 2.3, formalizing some concepts, such as frames, format and blocks. We also present the 1D applications of the method, described by Gutowitz & Victor (1987), using the bayesian extension process (FUKŠ, 2012).

In section 2.4, we describe our Automated Extension algorithm for building approximations for the extended frames, that reduces to the 1D application but allows us to build approximations for other lattices using the same core concepts, and discuss some problems that may arise from the algorithm used, in section 2.4.1. We follow with section 2.5, implementing the algorithm step-by-step in an example. In section 2.6, we briefly discuss some adjustments to reduce program runtime.

In section 2.7, we compare the performance of different approximations for the weak PD in a square lattice, using as a basis the MC simulations, in a similar manner to what was done by Szabo & Toke (1998), but we focus on the different options of extended frames. We find that with the right selection, not only can we reduce the program runtime, but we also improve the approximation made for the system. Based on observation, we briefly describe guidelines for choosing the extended frame in section 2.7.4.

2.1 A First Step: the Mean-field Approach

As a didactic introduction to the Local Structure Theory, we will show the Mean-Field Theory (MFT) and how its assumption fails to capture important features of the system we are trying to analyze. The basic assumption of MFT is that there is no correlation between neighbours, so that the probability of a given configuration being in a lattice is just the product of the independent sites being in their given states.

We will apply MFT to the following system: players in a square lattice play a weak Prisoner's Dilemma with their first neighbours and themselves (there is auto-interaction), choosing randomly a pair of neighbours, one of them copies their neighbour with probability given by a function f of the difference of their payoffs. In MFT, the state of the system will be defined by the probability of finding the players in a certain state (playing a certain strategy). In this case, there are only two states: cooperator (C) and defector (D). The system will be defined by two variables $p_C(t)$ and $p_D(t)$. These variables represent the probabilities of finding a cooperator and a defector, respectively. Using a normalization condition ($p_C + p_D = 1$), the state of the system can be defined using a single independent variable. We will adopt p_C for defining the system state and write a differential equation for the evolution of the system.

The system can change states when the randomly chosen neighbours form a cooperator-defector (CD) pair. The process of a cooperator invading a defector ($C \rightarrow D$) depends on the number of cooperating neighbours of each player (to calculate their payoff). In this case, the payoff difference between C and D will be $\Delta Pay(n_C, n_D) = (n_C + 1) - b(n_D + 1)$, where n_C (n_D) is the number of cooperating neighbours of the C (D) player excluding the initial pair considered (the C player gains +1 for playing with itself and the D player gains + b due to playing with the C). The probability of the C or D player having n cooperator neighbours (besides the one in the pair), $P(n, p_C)$ follows a binomial distribution:

$$P(n, p_C) = \binom{3}{n} p_C^n (1 - p_C)^{3-n}, \quad (2.1)$$

where the $\binom{3}{n}$ counts the different way we can arrange the n cooperators around the player, $p_C^n p_D^{3-n}$ the probability of having n cooperator and $3 - n$ defector neighbours, and all the three are due to the player having 3 neighbours beside the neighbour in the pair.

So, the probability of the C player having n_C cooperator neighbours, and, simultaneously, the D player having n_D cooperator neighbours, $P(n_C, n_D, p_C)$, is

$$P(n_C, n_D, p_C) = P(n_C, p_C)P(n_D, p_C) = \binom{3}{n_C} \binom{3}{n_D} p_C^{n_C+n_D} (1 - p_C)^{6-(n_C+n_D)}, \quad (2.2)$$

where p_C is the probability of a player being in the cooperator (C) state and the probability of being a defector (D) is $p_D = 1 - p_C$. We highlight that $P(n_C, n_D, p_C) = P(n_D, n_C, p_C)$,

meaning that this function is symmetrical under a $n_C \leftrightarrow n_D$ transformation. This means that in this estimation of the probability of the sites around the C and D pair, we can swap them from places and the probability of that configuration remains the same.

The change in the probability of finding cooperators (\dot{p}_C) is given by the difference between the rate of defectors invading cooperators ($N_{D \rightarrow C}$) and the rate of cooperators invading defectors ($N_{C \rightarrow D}$):

$$\dot{p}_C = (N_{C \rightarrow D} - N_{D \rightarrow C}) p_C(1 - p_C), \quad (2.3)$$

where $p_C(1 - p_C)$ is the probability of the central CD pair existing in the first place. This term guarantees that when $p_C = 1$ or $p_C = 0$, then $\Delta p_C = 0$, since there is no strategy update/change once one of the strategies becomes extinct. Considering that $p_C(1 - p_C)$ is strictly greater than 0 in the region $(0, 1)$, we will not be writing it in the following equations due to space limitation and the fact that it does not change the behaviour of the system, and can be considered a nonlinear rescale of time (HAUERT; SZABO, 2005).

To calculate the probability $N_{C \rightarrow D}$, we can sum the probability of a change occurring in a given configuration multiplied by the probability of that change, given by the $f(\Delta Pay(n_C, n_D))$:

$$N_{C \rightarrow D} = \sum_{n_C=0}^3 \sum_{n_D=0}^3 f(\Delta Pay(n_C, n_D)) P(n_C, n_D, p_C); \quad (2.4)$$

in the same manner for $N_{D \rightarrow C}$, only the probability of change is given by $f(-\Delta Pay)$:

$$N_{D \rightarrow C} = \sum_{n_C=0}^3 \sum_{n_D=0}^3 f(-\Delta Pay(n_C, n_D)) P(n_C, n_D, p_C) \quad (2.5)$$

$$= \sum_{n_C=0}^3 \sum_{n_D=0}^3 f(-\Delta Pay(n_D, n_C)) P(n_C, n_D, p_C), \quad (2.6)$$

where from equation (2.5) to (2.6), we simply rewrite the labels in the summation and use that $P(n_C, n_D, p_C) = P(n_D, n_C, p_C)$. Using the equations above to obtain the change in cooperators probability (\dot{p}_C), we obtain:

$$\dot{p}_C = \sum_{n_C=0}^3 \sum_{n_D=0}^3 [f((n_C + 1) - b(n_D + 1)) - f(b(n_D + 1) - (n_C + 1))] P(n_C, n_D, p_C) \quad (2.7)$$

$$= \sum_{n_C=0}^3 \sum_{n_D=0}^3 [f((n_C + 1) - b(n_D + 1)) - f(b(n_C + 1) - (n_D + 1))] P(n_C, n_D, p_C), \quad (2.8)$$

where we use equation (2.6) to write (2.8), so that it is evident that in the case where $b = 1$, $\dot{p}_C = 0$ as the term between square brackets becomes null. This means that for $b = 1$, the system does not change from the initial condition, and that all states are fixed points (but they are not really attractors). And we use equation (2.5) to write (2.7), so

we can analyze other values of b by differentiating \dot{p}_C in relation to b and, using the chain rule, we obtain:

$$\frac{d\dot{p}_C}{db} = \sum_{n_C=0}^3 \sum_{n_D=0}^3 (-n_D - 1) \left[\left. \frac{df(x)}{dx} \right|_{\Delta Pay(n_C, n_D)} + \left. \frac{df(x)}{dx} \right|_{-\Delta Pay(n_C, n_D)} \right] P(n_C, n_D, p_C). \quad (2.9)$$

It is easy to assume that f is a non-decreasing function, since for an increase in the payoff difference, it is expected that the change of being copied increases, or is at least the same. Given that $\frac{df}{dx} \geq 0$ results in $\frac{d\dot{p}_C}{db} \leq 0$ and that $\dot{p}_C = 0$ for $b = 1$ and the fair assumption that $\frac{df}{dx} > 0$ for some value¹, we can conclude that:

- For $b > 1$, $\dot{p}_C < 0 \forall p_C \in (0, 1)$. Meaning that if there is at least one defector in the system, they will come to dominate the whole system ($p_C = 0$ is a stable attractor).
- For $b < 1$, $\dot{p}_C > 0 \forall p_C \in (0, 1)$. Meaning that if there is at least one cooperator in the system, they will come to dominate the whole system ($p_C = 1$ is a stable attractor).

Excluding the $b = 1$ case, there is no stable coexistence of cooperators and defectors. However, this is a feature that appears when simulating this system with Monte Carlo (see section 2.7). Therefore, this approximation fails to capture an essential feature of the system. In the next section, we will include local pair correlations to better predict the system behavior, and later on we will show how to generalize to include more extensive local correlations.

2.2 Local pair correlations approach

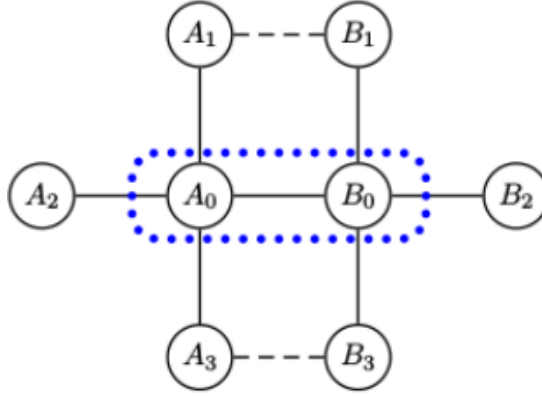
In this approach, we will assume that the system evolution does not build correlations larger than neighbour-to-neighbour (pairwise) correlations. We will call a pair of players a “ $S_1 S_2$ pair” when one of the neighbours uses strategy S_1 and the other uses strategy S_2 . We will consider the same system of the previous section (a weak PD in a square lattice with interaction). In this approximation, there will be four variables that define the state of the system: the probability of finding each of the pairs in the lattice: p_{CC} , p_{CD} , p_{DC} , p_{DD} , which are, respectively, the probability of finding the pair CC , CD , DC , DD . These probabilities meet certain conditions:

- **Normalization:** The function must be normalized ($p_{CC} + p_{CD} + p_{DC} + p_{DD} = 1$) to be interpreted as probability.

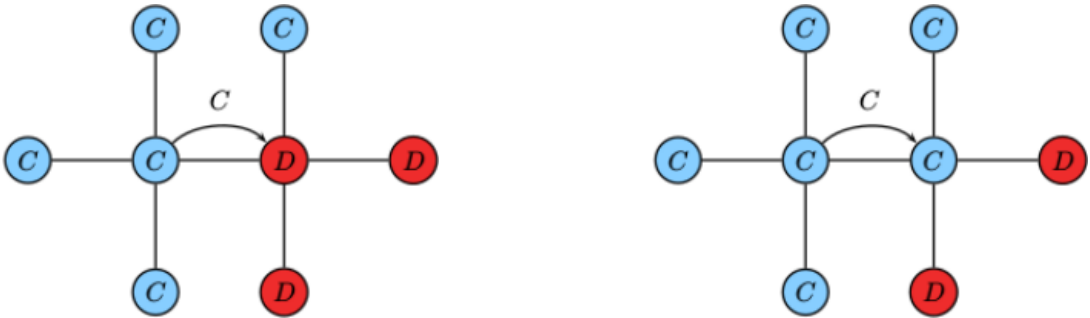
¹ It is evident that $\Delta f > 0$ for some value of Δx (for f not constant in the region of payoff differences). Although this does not prove the assumption that $\frac{df}{dx} > 0$ for some of the x value assumed in our summation, it is enough for the presented conclusion.

- **Symmetry under rotation:** Since the square lattice is symmetrical under $\pi/2$ rotations and the process does not have directional preference, the equality $p_{CD} = p_{DC}$ must hold. Due to this, we will use CD and DC interchangeably.
- **Closure condition:** the probability of a single player being in a given state can be obtained by $P_{\circ}(C) = p_{CC} + p_{CD}$ (probability of a site being in a state C) and $P_{\circ}(D) = p_{DC} + p_{DD}$ (probability of a site being in a state D).

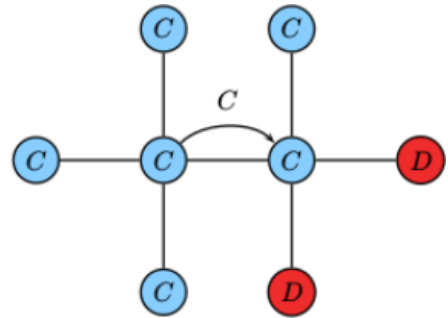
The normalization and symmetry under rotation conditions reduce the number of free independent variables from four to two. Different than the previous approach where setting $P_{\circ}(C)$ fully determined the state of the system, we will have to set two variables: $P_{pair}(CC)$ and $P_{pair}(CD)$ or $P_{pair}(CC)$ and $P_{pair}(DD)$, for example. Another set of variables is considered further in this section. In a similar manner to the last section, the evolution of the system will also be determined by differential equations for these variables.



(a) A generic configuration $(A_0B_0)A_1A_2A_3B_1B_2B_3$ on the pair frame. Changes (processes) only happen inside the blue dotted box. For now, we will disregard the A_1B_1 and A_3B_3 connections (dashed lines) when estimating this block probability.



(b) Before the $C \rightarrow D$ invasion (configuration (CD)CCCCDD).



(c) After the $C \rightarrow D$ invasion (configuration (CC)CCCCDD).

Figure 1 – The pair frame with a generic configuration (a), and a specific configuration before (b) and after (c) a $C \rightarrow D$ invasion process.

Before trying to write the equations for the evolution of the system, we will analyze a specific configuration and what happens when there is a C invading a D . In Figure 1b,

we are considering a cooperator with 3 cooperator neighbours invading a defector site with only one cooperator neighbour and two defector neighbours. In Figure 1c, we see the configuration after the D player changes to a C player. We can observe that two CD pairs change to CC pairs and two DD pairs change to CD pairs due to the invasion. Therefore, the total number of CD pairs does not change, while the number of CC (DD) pair increases (decreases) by two. When this process happens, it changes the probability of CC pairs (p_{CC}) and DD pairs (p_{DD}). The contribution of this exact process to \dot{p}_{CC} would be 2 multiplied by the probability of the process happening (ω) multiplied by the probability P_{config} of this specific eight-site configuration presented in Figure 1a happening in the lattice:

$$\frac{dp_{CC}}{dt} = 2\omega P_{config}((CD)CCCCDD) + \text{other contributions.} \quad (2.10)$$

Different from $\frac{dp_{CC}}{dt}$, for $\frac{dp_{CD}}{dt}$ the contribution of this specific process is null, as the number of the CD pairs do not change, the contribution for $\frac{dp_{DD}}{dt}$ is the negative of that for $\frac{dp_{CC}}{dt}$.

We can estimate the probability of these configurations using the probability of the pairs in a similar manner to what was done in the previous section. However, in this one, we multiply the probability of all pairs in the configuration before the invasion. Ignoring the connections between A_1B_1 and A_3B_3 , we can count three CC , two CD , two DD pairs, and obtain the following probability:

$$P_{config}((CD)CCCCDD) = \frac{p_{CD}}{P_o^3(C) P_o^3(D)} p_{CC}^3 p_{CD} p_{DD}^2, \quad (2.11)$$

where we divide by the site probabilities P_o , because the central sites appear four times in the pair probabilities. A visual representation of P_{config} can be seen in Figure 2. This also normalizes the P_{config} function:

$$\sum_{\substack{A_1, A_2, A_3, \\ B_1, B_2, B_3 \\ = (C, D)}} P_{config}((CD)A_1A_2A_3B_1B_2B_3) = \frac{p_{CD}}{P_o^3(C) P_o^3(D)} \prod_{i=1}^3 \left[\sum_{A_i} p_{CA_i} \right] \left[\sum_{B_i} p_{CB_i} \right] \quad (2.12)$$

$$= \frac{p_{CD}}{P_o^3(C) P_o^3(D)} \prod_{i=1}^3 P_o(C) P_o(D) = p_{CD}, \quad (2.13)$$

where, in the second equality, we are using the closure condition.

In order to write the evolution equations, we have to consider that each player in $j = \{A_1A_2A_3B_1B_2B_3\}$ can be a cooperator (C) or a defector (D). Then, we should sum the contribution of all processes that can happen in all different configurations in the eight-site frame presented in Figure 1a. The contribution is weighted by the probability ω_χ^j that the given process happens for configuration j and also weighted by the number of pair changes the process χ causes, that can be encoded in a function $(\Delta N_a)_{\chi, (CD)j}$.

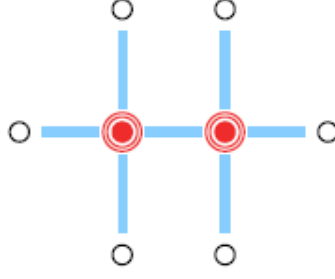


Figure 2 – Visual representation of the estimated probability P_{config} of the eight-site configuration. Blue painted structures means the term enters multiplying and red painted structures enters the approximation dividing, extra red circles around a site means dividing more times.

For the example in Figure 1b, where the process is $C \rightarrow D$ and the configuration is $(CD)CCCCDD$, this function would be:

$$\begin{aligned}
 (\Delta N_{CC})_{C \rightarrow D, (CD)CCCCDD} &= +2 ; \\
 (\Delta N'_{CD})_{C \rightarrow D, (CD)CCCCDD} &= 0 \leftarrow \begin{cases} (\Delta N_{CD})_{C \rightarrow D, (CD)CCCCDD} = +1 ; \\ (\Delta N_{DC})_{C \rightarrow D, (CD)CCCCDD} = -1 ; \end{cases} \\
 (\Delta N_{DD})_{C \rightarrow D, (CD)CCCCDD} &= -2 . \tag{2.14}
 \end{aligned}$$

In this case, we are considering $(\Delta N'_{CD}) = (\Delta N_{CD}) + (\Delta N_{DC})$ and, later $\Delta N'_{CD}$ will be divided by two. The numbers are equal for both CD and DC pairs because we are considering a process that is symmetrical in the lattice. For each process in a given configuration changing n CD pairs and m DC pairs there will be a “mirrored” configuration, where the “mirrored” process changes m CD and n DC pairs.

Based on that, we can write the evolution equation for p_{CC} and p_{CD} , and, in this way, fully describe the evolution of the variables as:

$$\frac{dp_{CC}}{dt} = 2p_{CD} \sum_j \left(\frac{p_{CA_1} p_{CA_2} p_{CA_3} p_{DB_1} p_{DB_2} p_{DB_3}}{P_{\circ}^3(C) P_{\circ}^3(D)} \sum_{\chi} \omega_{\chi}^{(CD)j} (\Delta N_{CC})_{\chi, (CD)j} \right) ; \tag{2.15}$$

$$\frac{dp_{CD}}{dt} = 2p_{CD} \sum_j \left(\frac{p_{CA_1} p_{CA_2} p_{CA_3} p_{DB_1} p_{DB_2} p_{DB_3}}{P_{\circ}^3(C) P_{\circ}^3(D)} \sum_{\chi} \omega_{\chi}^{(CD)j} \frac{(\Delta N'_{CD})_{\chi, (CD)j}}{2} \right) ; \tag{2.16}$$

where the summation in χ represents the processes $C \rightarrow D$ and $D \rightarrow C$. The number 2 multiplying both equations (2.15) and (2.16) comes from the contributions from a centralized DC pair instead of a CD pair, that would result in an equal contribution for the way the $(\Delta N')$ was defined. It also does not change the dynamics as t is being very loosely defined and a multiplicative term in all differential equation does not change the evolution path. The 2 in the denominator in equation (2.16) is also due to the way we defined (ΔN) , specially (ΔN_{CD}) , and can be justified by deriving the normalization condition $(\frac{d(p_{CC} + p_{CD} + p_{DC} + p_{DD})}{dt} = 0)$.

We can write (ΔN) as a function of the number of cooperator neighbours of the invaded pair (basically, n_C and n_D defined in the last section):

$$(\Delta N_{CC})_{C \rightarrow D} = 1 + n_D ; \quad (\Delta N_{CC})_{D \rightarrow C} = -n_C ; \quad (2.17)$$

$$(\Delta N'_{CD})_{C \rightarrow D} = 2(1 - n_D) ; \quad (\Delta N'_{CD})_{D \rightarrow C} = 2(n_C - 2) . \quad (2.18)$$

For the curious, we open equations (2.15) and (2.16) for the specific case of the system with self-interaction and temptation value $b = 1.5$, and transition function ω being a Fermi function (defined in Appendix D) with parameter $K = 0.1$:

$$\begin{aligned} \frac{dp_{CC}}{dt} = & p_{CD}^3 p_{DD}^3 + 0.04 p_{CD}^4 p_{DD}^2 + 3 p_{CC} p_{CD}^2 p_{DD}^3 + 17.82 p_{CC} p_{CD}^3 p_{DD}^2 - 9 p_{CC} p_{CD}^4 p_{DD} + \\ & - 3 p_{CC} p_{CD}^5 + 3 p_{CC}^2 p_{CD} p_{DD}^3 + 18 p_{CC}^2 p_{CD}^2 p_{DD}^2 + 4.5 p_{CC}^2 p_{CD}^3 p_{DD} - 6 p_{CC}^2 p_{CD}^4 + \\ & + p_{CC}^3 p_{DD}^3 + 6 p_{CC}^3 p_{CD} p_{DD}^2 + 9 p_{CC}^3 p_{CD}^2 p_{DD} - 2.95 p_{CC}^3 p_{CD}^3 . \end{aligned} \quad (2.19)$$

$$\begin{aligned} 2 \frac{dp_{CD}}{dt} = & 2 p_{CD}^3 p_{DD}^3 - 11.92 p_{CD}^4 p_{DD}^2 - 12 p_{CD}^5 p_{DD} - 4 p_{CD}^6 + 6 p_{CC} p_{CD}^2 p_{DD}^3 + \\ & - 0.12 p_{CC} p_{CD}^3 p_{DD}^2 - 18 p_{CC} p_{CD}^4 p_{DD} - 6 p_{CC} p_{CD}^5 + 6 p_{CC}^2 p_{CD} p_{DD}^3 + \\ & - 9 p_{CC}^2 p_{CD}^3 p_{DD} + 2 p_{CC}^3 p_{DD}^3 - 6 p_{CC}^3 p_{CD} p_{DD} + 1.96 p_{CC}^3 p_{CD}^3 . \end{aligned} \quad (2.20)$$

Obviously, equations (2.19) and (2.20) convey little to no information for the reader, but may be useful for comparison when trying to recreate this specific case. For a better readability of these equations, we visually represent these vector fields in Figure 3, using streamlines.

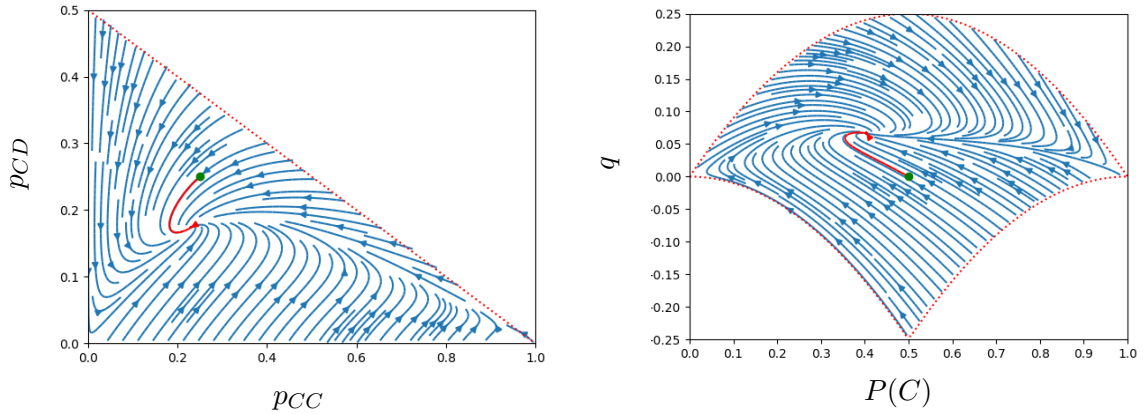
For comparison effects, and as an example, we will use another set of independent variables that are suggested in Szabo & Fath (2007, p. 203). Instead of using p_{CC} and p_{CD} as our variables, we will use the probability of a player being a cooperator ($P_o(C) = P(C)$) and a measure of deviation from the well-mixed state (q):

$$p_{CC} = P^2(C) + q ; \quad P(C) = p_{CC} + p_{CD} ; \quad (2.21)$$

$$p_{CD} = P(C)(1 - P(C)) - q ; \quad q = p_{CC} - (p_{CC} + p_{CD})^2 ; \quad (2.22)$$

where the conditions for p to be interpreted as a probability function are stated in our new variables as $\{0 \leq P(C) \leq 1\}$ and $\{-\min\{P^2(C), (1 - P^2(C))\} \leq q \leq [1 - P(C)]P(C)\}$. Time derivatives for $P(C)$ and q could be obtained in terms of the derivatives of p_{CC} and p_{CD} through direct derivation of expressions in (2.21) and (2.22).

In both streamline maps of Figure 3, we can clearly observe a stable attractor point in $(p_{CC}, p_{CD}) \approx (0.233, 0.172)$ (equivalent to $(P_C, q) \approx (0.405, 0.065)$). Therefore, using this approximation, we can see a coexistence of cooperator and defectors. This result presents, at least, a qualitative improvement upon the mean-field result presented in section 2.1, since coexistence of cooperator/defector is a feature present in Monte Carlo simulations. In later sections, we will compare these and other approximations more



(a) Graph using p_{CC} and p_{CD} as variables. (b) Graph using $P(C)$ and q as variables.

Figure 3 – The streamline graphs shows the vector field determined by equations (2.19) and (2.20). As we can see, there is a stable attractor point (marked by the red triangle) at $(p_{CC}, p_{CD}) \approx (0.233, 0.172)$ in the first graph, or in the equivalent position in the second graph at $(P_C, q) \approx (0.405, 0.065)$. The dotted red line marks the upper limit due to the normalization condition and non-negativity of the probability function p . The green dots marks $(p_{CC}, p_{CD}) = (0.25, 0.25)$ (alternatively, $(P_C, q) = (0.5, 0)$) the well-distributed (half cooperator/half defector) state that is generally assigned at start of MC simulations. The continuous red line marks the evolution path (streamline) to the attractor point.

minutely. We will in the next sections describe how to generalize this “correlation method” for other lattices, for more extensive correlations and discuss different approximations based on this method.

2.3 Local Structure Theory

Local Structure Theory (LST) was initially designed to mathematically treat cellular automata on one-dimensional lattices (GUTOWITZ; VICTOR; KNIGHT, 1987), and was later extended to Euclidean lattices (GUTOWITZ; VICTOR, 1987; GUTOWITZ; VICTOR, 1994); applications in evolutionary Game Theory (SZABO; TOKE, 1998) and other areas followed (DICKMAN, 1988; DICKMAN, 1990; HIEBELER, 1997). The basic assumption of LST is that the correlations generated by the system decay with distance and that, with this assumption, we can estimate the probability of larger blocks based on the probability of the smaller blocks it contains. We will make some definitions in Subsection 2.3.1 and explain the case of one-dimension in subsection 2.3.3 so that explaining the general method developed to build the approximation, described in Section 2.4, becomes easier.

2.3.1 Definitions: Frame, Frame Format, Block

In this section, we introduce the frame and block concepts presented in [Gutowitz & Victor \(1987\)](#) in a simple and comprehensive manner. Our definitions vary from the original, in being a little loose so we can adapt it to different systems.

A simple way to think of a **frame** is to think of it as, given a lattice or graph and an ordered list of sites, the graph formed only by the sites from this list. A more elaborate and workable definition is that the **frame** is an object that contains the “connection properties” (in an orderly form) of an ordered list (that is, a tuple) of sites in a lattice or graph. The “connection properties” are very loosely defined on purpose, because different systems may need different concepts of “connection properties”. For example, a system that breaks isometry may need definitions of relative position, like site E is the left neighbour of site F , rather than just knowing they are neighbours. This loose definition allow us to describe a method for building approximations that can be later adapted for a multitude of systems. One way to define the “connection properties” could be by defining the number of paths of size n that go from site E to F in the lattice (E, F in the tuple forming the frame). The number of paths of size 1 is the Adjacency matrix A between the sites in the tuple and it will be the only information needed for some cases. Other cases may require more information. In section 2.2, we have loosely used “pair” frames and an eight-site frame, which can not be formed from a square lattice, since it is missing some connections. For a visualization of the frame, we could use the graphs formed by sites, as exemplified for different frames in Figure 4.

Another example, set in the square lattice, is that we can form a frame f from the ordered tuple $[(0, 0), (0, 1), (1, 0), (1, 1)]$ and a frame g from the tuple $[(1, 0), (1, 1), (2, 0), (2, 1)]$. The frames f and g have the same “connection properties” between the sites (in their given position in the tuple), and we will say that f and g have the **same frame format** (or shape). In Figure 4c, the frames formed by $[A_0, B_0, A_1, B_1]$ and $[A_0, B_0, A_3, B_3]$ have the same frame format, also the pair frames $[A_0, B_0]$ and $[A_1, B_1]$ in Figure 4b have the same frame format. We will generally call a frame format by the figure it represents in the lattice. For example, the frame format of f is a square, a visual representation in Figure 4a.

Another concept we will use is the **permuted frame**, which is a frame generated by a permutation of the elements in the tuple. For example, the frame generated by the tuple $[A_1, B_1, A_0, B_0]$ has the same frame format as $[A_0, B_0, A_1, B_1]$, but the frame generated by $[A_0, B_0, B_1, A_1]$ does not have the same frame format. Although both are permutations of the first tuple presented, the second one does not have the same “connection properties” (the second site is a direct neighbour with the third which doesn’t happen in the original). In general, we will consider only one of the permutations of a frame when searching for frames that have a certain format/shape. For example, we considered

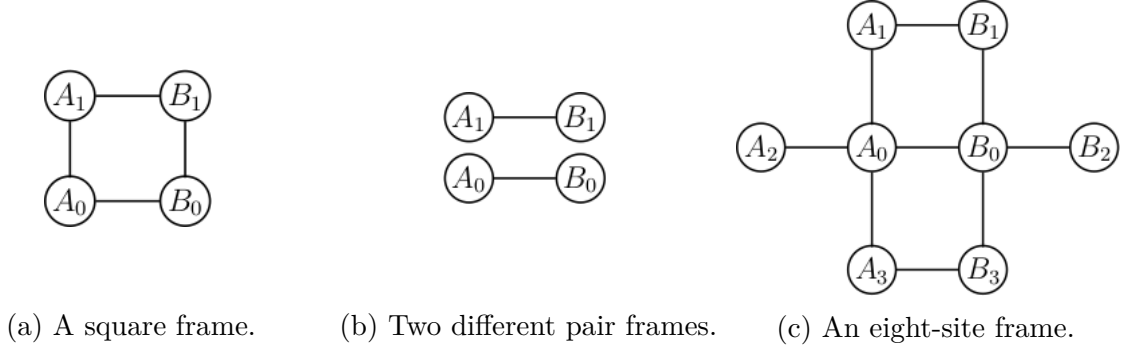


Figure 4 – Visualization of different frames.

the pair CA_1 and ignored the pair A_1C in section 2.2.

Another related concept is a **subframe**. A frame f is a subframe of g , when the tuple that forms f can be formed by the removal of sites from the tuple that forms g . For example, the square frame in Figure 4a is a subframe of the eight-site frame in Figure 4c, and the pair frames in Figure 4b are subframes of the square frame and, consequently, of the eight-site frame.

Finally, a **block** is the assignment of states to all players in a frame or frame format. For example, $\{CD, CC, DD, DC\}$ are all blocks in the pair frame, used in the section 2.2. To simplify the notation, the set of all blocks for a given frame format will be called σ_{format} . We can define a function $P_{format}(X)$ that represents the probability for a given frame of that format to be an X block. For example, $P_{pair}(CD)$ would be the probability that a pair in the system is a CD block. For $P_{format}(X)$ to be a probability function, the function must be non-negative,

$$\{P_{format}(X) \geq 0\} \quad \forall X \in \sigma_{format} , \quad (2.23)$$

and normalized,

$$\sum_{X \in \sigma_{format}} P_{format}(X) = 1. \quad (2.24)$$

There will be block probabilities, generally connected to a specific frame format, that we will be directly updating when performing the evolution of the system. Generally, to make notation less extensive, we will use $p_X \equiv P_{format}(X)$, making it easier to identify and write equations. For example, in section 2.2, we have used $p_{CD} = P_{pair}(CD)$. We will call the blocks we are updating as **central** blocks, or **important** blocks, to differentiate from other blocks. These same adjectives will be used for the frame or frame format underlying theses blocks.

Generally, in Game Theory and also in Cellular Automata, the changes to a player state depends on its neighbours state. Consequently, defining only the configuration in a frame is not necessarily enough to define the dynamics of that frame. Therefore, we will need to be able to estimate the probability of a larger frame, including the neighbours

of the initial frame. In the pair approximation example, in section 2.2, we constructed an extended frame, shown in Figure 1a, containing the other three neighbours for each player of the pair, in a total of eight players in this extended frame and we estimated its blocks probabilities using equation (2.11).

Our central block probabilities will be updated over time by the equation (2.25), which is calculated using the different configurations in those extended frames and processes that can happen in those frames:

$$\dot{p}_i = \sum_{j \in \sigma_{ext}} \left[P_{ext}(j) \left(\sum_{\chi} \omega_{\chi}^j (\Delta N_i)_{j,\chi} \right) \right], \quad (2.25)$$

where $P_{ext}(j)$ is the probability of a j extended block in the extended frame; ω_{χ}^j is the probability of process χ happening in a j extended block; and $(\Delta N_i)_{j,\chi}$ is the change counting function for the i (central) block, that counts how many i (central) blocks are created subtracted by how many are modified to other blocks if the χ process happens in the j extended block. The ω and ΔN_i are described by the model we are considering (game, lattice, method of update...) and are independent of the particular probabilities of blocks. We will use the central block probabilities $\{p_i\}$ to construct $P_{ext}(j)$. We indicate section 2.2, again, as an exemplification of the defined functions ω , ΔN and P_{ext} (in that case P_{config} above, the equations (2.15) and (2.16) are specific cases of (2.25).

Equation (2.25) will always maintain the original normalization of the block probabilities as $\sum_i (\Delta N_i)_{j,\chi} = 0$, since there is no “creation” of new blocks, only transformations from one type of block into another. In this way, we can show that the normalization of the block probability is preserved:

$$\frac{d}{dt} \left(\sum_i p_i \right) = \sum_i \dot{p}_i = \sum_{j \in \sigma_{ext}} \left[P_{ext}^{(j)} \left(\sum_{\chi} \omega_{\chi}^j \sum_i (\Delta N_i)_{j,\chi} \right) \right] = 0. \quad (2.26)$$

This is important, as P_{ext} may be constructed as a non-normalized function and the original/central $p = P_{frame}$ function will still remain normalized.

2.3.2 Closure condition and probability for smaller blocks

Using the block probability for a frame f , we can estimate the block probabilities for a frame g , a subframe of f . We will name L_{f-g} as the list of the members of f removed to form g and L_g as the list of member of g . To obtain the probability for a given s block of g , we can realize the following summation over all possible states (blocks) of the members L_{f-g} ($\sigma_{L_{f-g}}$):

$$P_g(s) = \sum_{i=\text{state of } L_{f-g}}^{\sigma_{L_{f-g}}} P_f(s+i); \quad (2.27)$$

where $s+i$ is a block of f , which we attributed the s states to the members of L_g and the i states to the L_{f-g} , according to their positions in the f frame. In general, we will call this a closure condition of P_f .

For example, if we have pair block probabilities (p_{pair}) and we want to obtain the probability for single site being in state s , $P_o(s)$, we would simply sum over all pair probabilities, where the first point is in state s :

$$P_o(s) = \sum_i P_{pair}(s, i). \quad (2.28)$$

Another example is obtaining the probability function for pair blocks (P_{pair}) given that we have square block probabilities (P_{square}):

$$P_{pair}(s_1, s_2) = \sum_{i,j} P_{square}(s_1, s_2, i, j) = \sum_{i,j} P_{square}(s_1, j, i, s_2); \quad (2.29)$$

where the player in state s_1 neighbours the ones playing s_2 and j ; the other connections are self-evident.

In all cases, it is clear that the normalization of the constructed probability function for the subframe follows the normalization for the extended frame.

2.3.3 Approximation of the probability of larger blocks in one dimension

The important point of Local Structure Theory is presenting an approximation for the probability of larger blocks from the smaller blocks it contains. Its base is the bayesian extension process. In the one dimension (1D) case, we will be interested in the probabilities of n connected, sequential, players. The LST, according to [Gutowitz, Victor & Knight \(1987\)](#), allows the estimation of a n -block probability (P_n) from the probabilities of two $(n - 1)$ -blocks (P_{n-1}) by

$$P_n(s_1, s_2, \dots, s_{n-1}, s_n) = \frac{P_{n-1}(s_1, s_2, \dots, s_{n-1})P_{n-1}(s_2, \dots, s_{n-1}, s_n)}{P_{n-2}(s_2, \dots, s_{n-1})}, \quad (2.30)$$

where P_{n-2} can be constructed using the closure condition exemplified in the last section, and defining P_0 for the empty set (\emptyset): $P_0(\emptyset) = 1$.

We can see in (2.30) that the term that appears dividing refers to the $(n - 2)$ block that appears in the two $(n - 1)$ -blocks probabilities being multiplied. We can demonstrate that the constructed P_n function will be normalized if P_{n-1} and, consequently, P_{n-2} are:

$$\sum_{s_1, \dots, s_n} P_n(s_1, \dots, s_n) \quad (2.31)$$

$$= \sum_{s_2, \dots, s_{n-1}} \frac{1}{P_{n-2}(s_2, \dots, s_{n-1})} \left(\sum_{s_1} P_{n-1}(s_1, \dots, s_{n-1}) \right) \left(\sum_{s_n} P_{n-1}(s_2, \dots, s_n) \right) \quad (2.32)$$

$$= \sum_{s_2, \dots, s_{n-1}} \frac{1}{P_{n-2}(s_2, \dots, s_{n-1})} P_{n-2}(s_2, \dots, s_{n-1}) \cdot P_{n-2}(s_2, \dots, s_{n-1}) \quad (2.33)$$

$$= \sum_{s_2, \dots, s_{n-1}} P_{n-2}(s_2, \dots, s_{n-1}) = 1, \quad (2.34)$$

where, in the second equality, the summation in parenthesis is exactly the closure condition that describes P_{n-2} . In the last equality, we used the fact that P_{n-2} is normalized.

We can use the definition in equation (2.30), recurrently, to estimate an n -block probability from an $(n-2)$ -block probabilities and so on. In the example of estimating a n -block probability with $(n-2)$ -block probabilities, we would end up with the equation

$$P_n(s_1, s_2, \dots, s_{n-1}, s_n) = \frac{P_{n-2}(s_1, \dots, s_{n-2}) \cdot P_{n-2}(s_2, \dots, s_{n-1}) \cdot P_{n-2}(s_3, \dots, s_n)}{P_{n-3}(s_2, \dots, s_{n-2}) \cdot P_{n-3}(s_3, \dots, s_{n-1})}. \quad (2.35)$$

This would be an approximation using shorter correlations to estimate the n -block probability.

Using the equation (2.30) recurrently $(n-1)$ times, we would end up with

$$P_n(s_1, s_2, \dots, s_{n-1}, s_n) = \prod_{j=1}^n P_1(s_j) = P_1(s_1) \cdot P_1(s_2) \dots P_1(s_{n-1}) \cdot P_1(s_n), \quad (2.36)$$

where this would be the estimation based on the assumption that there is no correlation between players. This is equivalent to the common mean-field approximation for the one dimensional case, where we would have just the site probability to estimate the probability of a larger sequence of players in the network.

2.4 Automated Extension Algorithm

The LST approximation is easily applied for one dimension and acyclic graphs. However naturally extending this process to more dimension or more complex structures may be hard, as is explained by [Gutowitz & Victor \(1987\)](#):

In more than one dimension maximum entropy extension is considerably more delicate. The variational problem translates into a system of polynomial equations, whose explicit solution in terms of radicals is in general not possible. Furthermore, extension to each larger frame typically requires solution of an entirely new (and larger) system of equations. In this paper we do not solve the more general problem. Rather, we approximate the maximum entropy extension by a formula which is a straight-forward analog of the one-dimensional formula. As in the one dimensional case, the formula is rational in smaller block probabilities. ([GUTOWITZ; VICTOR, 1987](#), p. 59)

With the same idea, but focusing on the ease of implementation, we propose and describe a simple algorithm for building these approximations, inspired by the Bayesian extension process, which is both simple to implement and whose motivations are simple to explain.

As a guideline for the automated extension process, we do not want any player (and, in general, structures smaller than the considered central frame) in the extended

frame probability function to be over or underrepresented. For that, the number of times it appears in the numerator minus the number of times it appears in the denominator must be equal to one. For example, in equation (2.30), the s_1 and s_n both appear once in the numerator, while s_2, \dots, s_{n-1} appear twice in the numerator and once in the denominator. We also want to use the correlations to a maximum when correcting an over or underrepresentation. For example, in equation (2.30), we divide by a P_{n-2} block probability and not by $n - 2$ P_1 block probabilities, since $P_{n-1}(s_1, \dots, s_{n-1})$ and $P_{n-1}(s_2, \dots, s_n)$ “share” the $n - 2$ players (s_2, \dots, s_{n-1}) .

Keeping the concept of over or underrepresentation in mind, we created a simple algorithm to determine how many times we should multiply/divide a certain (smaller) block probability to estimate the probability for the extended block:

0. Input: The extended frame (N_{ext} sites) and central frame format (with N_{cen} sites).
1. First, identify all frames (non-permuted) with the same format as the desired central frame contained in the extended frame. Define the set of these frames as Φ_0 and the number of frames in this set as m_0 . The multiplication of those central block probabilities form the first part of the approximation, so define $c_0[i] = 1 \forall i \in [1, m_0]$.
2. Now, start to check if the subframes of the central frame are being over or underrepresented, starting at the ones with $N_{cen} - 1$ sites until the frames with one site (looping a variable R from 1 to $N_{cen} - 1$, with a step of 1):
 - a) Find all different frame formats of size $N_{cen} - R$. This is done by removing R members of the central frame and checking for different (non-permuted) frame formats.
 - b) Find all different frames (non-permuted) in those formats in the extended frame. This forms the set Φ_R and the number of frames in that set m_R . For each frame, start a variable $c_R[i] \leftarrow 1 \forall i \in [1, m_R]$.
 - c) For each frame f in Φ_R , check for a frame g of the sets $\Phi_0, \dots, \Phi_{R-1}$ (sets of larger frames). If f is a subframe of g , update the $c_R[f]$ subtracting the c value of that g frame ($c_R[f] \leftarrow c_R[f] - c_{n_g}[g]$, where n_g is N_{cen} minus the size of g).
 - d) Set the counter R to $R \leftarrow R + 1$.
3. The formula for the approximation of the extended block can then be written as:

$$P_{ext}(s) = \prod_{R=0}^{N_{cen}-1} \prod_{f \in \Phi_R} [P_f(s_f)]^{c_R[f]}, \quad (2.37)$$

where s_f is the block contained in the frame f , which is a sub-block of the total s (extended frame) block, and P_f is the block probability for the frame format of f .

We can check that this algorithm generates the approximation as described in equations (2.30) and (2.35) for the particular case of one dimension. And it also allows us to extend this approximation for other, more complex, structures and lattices.

The c_R variables will dictate how many times we divide or multiply by some frame in the extension probability. A $c_R(f) = 0$ means the frame f will not be used in calculating the extended probability. In step (2.c) we count how many times that frame is already multiplying and dividing the extended probability as subframes of a larger frame. This way, c_R counts the times a certain structure has been “represented” in the extension.

In the section 2.5, we will work with an example of a 3x4 extended frame approximated using a square format frame (four sites) to make the steps more clear to the reader. We will also discuss, in section 2.4.1, problems when trying to estimate the probability of cyclic structures using non-cyclic frames. Even in these cases, the approximation can be used as it was explained in equation (2.26), where we showed that the central block probabilities will remain normalized.

2.4.1 Problem with cyclic structures: Losing normalization and closure

When using the Automated Extension Process, we observed a problem in normalization when building some of the approximations. An example is when we try to estimate a square frame using pair frames. However, to simplify, we will exemplify with the simplest closed cyclic graph, which is a triangle, and analyze the problem in which we try to approximate its frame using pair frames. Using the Automated Extension Process for describing the probability of a triangle (P_Δ) in terms of the probability of pairs, we obtain:

$$P_\Delta(a, b, c) = \frac{p_{pair}(a, b)p_{pair}(b, c)p_{pair}(c, a)}{P_1(a) \cdot P_1(b) \cdot P_1(c)} . \quad (2.38)$$

Summing over all configurations, we can easily see that the normalization of P_Δ is lost, since

$$R = \sum_{j \in \sigma_\Delta} P_\Delta(j) = \sum_{a,b} \frac{p_{pair}(a, b)}{P_1(a) \cdot P_1(b)} \sum_c \frac{p_{pair}(b, c) p_{pair}(c, a)}{P_1(c)} \neq 1 , \quad (2.39)$$

unless there is no pair correlation, meaning $p_{pair}(i, j) = P_1(i) \cdot P_1(j) \forall i, j$, we would have:

$$\sum_{j \in \sigma_\Delta} P_\Delta(j) = \sum_{a,b} \frac{P_1(a) \cdot P_1(b)}{P_1(a) \cdot P_1(b)} \sum_c \frac{P_1(b) \cdot P_1(c) \cdot P_1(c) \cdot P_1(a)}{P_1(c)} \quad (2.40)$$

$$= \sum_a P_1(a) \sum_b P_1(b) \sum_c P_1(c) = 1 . \quad (2.41)$$

Even in the case where we renormalize P_Δ by dividing by a constant R , the problem persists in the fact that we do not obtain p_{pair} from P_Δ when summing one site out (closure

condition):

$$p_{pair}(a, b) \stackrel{?}{=} \sum_c \frac{P_{\Delta}(a, b, c)}{R} = \frac{1}{R} \frac{p_{pair}(a, b)}{P_1(a) \cdot P_1(b)} \sum_c \frac{p_{pair}(b, c)p_{pair}(c, a)}{P_1(c)} \quad (2.42)$$

$$R \stackrel{?}{=} \frac{1}{P_1(a) \cdot P_1(b)} \sum_c \frac{p_{pair}(b, c)p_{pair}(c, a)}{P_1(c)}. \quad (2.43)$$

With equation (2.43), we can see that the closure condition will not be met, unless R is a function of the states a, b (or, in the case where there is no pair correlation), which is incoherent with R being a constant. Consequently, it is evident that this approximation for the triangle frame is a little problematic. However, as we presented earlier in equation (2.26), constructing non-normalized probability approximations for external frames will not break the normalization for the probabilities we are updating.

In some cases, some pair relations are ignored when building the approximation (using $P_{\Delta}(a, b, c) = \frac{p_{pair}(a,b)p_{pair}(b,c)}{P_1(b)}$ would be an example). This would maintain the normalization but the approximation would have a worse performance, as we will show, in section 2.7.1, specifically when we compare the Simple and Connected pair approximations. The former represents the case where we ignore some connections and the latter presents the problems with normalization/closure presented in this section. In this particular case, the eight-site frame is a cyclic structure, which forms squares.

2.5 Code Implementation and Example of Application

For this code implementation, we will drop some of the generality from the definitions we have been using so far and work on one example: building an approximation for a 3x4 extended frame using a square as central frame format.

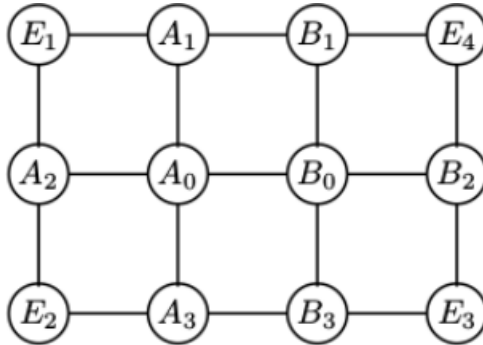


Figure 5 – Graph of the sites in the 3×4 Extended frame.

The extended frame for the $N = 12$ player will be defined by the $N \times N$ adjacency

matrix M_{ext} between the sites^{2,3}, which can also be visualized in graph form in Figure 5:

$$M_{ext} = \begin{matrix} & A_0 & B_0 & A_1 & A_3 & A_2 & B_1 & B_3 & B_2 & E_1 & E_2 & E_3 & E_4 \\ \begin{matrix} A_0 \\ B_0 \\ A_1 \\ A_3 \\ A_2 \\ B_1 \\ B_2 \\ B_3 \\ E_1 \\ E_2 \\ E_3 \\ E_4 \end{matrix} & \left(\begin{array}{cccccccccccc} - & 1 & 1 & 1 & 1 & 0 & 0 & 0 & 0 & 0 & 0 & 0 & 0 \\ 1 & - & 0 & 0 & 0 & 1 & 1 & 1 & 0 & 0 & 0 & 0 & 0 \\ 1 & 0 & - & 0 & 0 & 1 & 0 & 0 & 1 & 0 & 0 & 0 & 0 \\ 1 & 0 & 0 & - & 0 & 0 & 1 & 0 & 0 & 1 & 0 & 0 & 0 \\ 1 & 0 & 0 & 0 & - & 0 & 0 & 0 & 0 & 1 & 1 & 0 & 0 \\ 0 & 1 & 1 & 0 & 0 & - & 0 & 0 & 0 & 0 & 0 & 0 & 1 \\ 0 & 1 & 0 & 1 & 0 & 0 & - & 0 & 0 & 0 & 0 & 1 & 0 \\ 0 & 1 & 0 & 0 & 0 & 0 & 0 & - & 0 & 0 & 1 & 1 & 0 \\ 0 & 0 & 1 & 0 & 1 & 0 & 0 & 0 & 0 & - & 0 & 0 & 0 \\ 0 & 0 & 0 & 1 & 1 & 0 & 0 & 0 & 0 & 0 & - & 0 & 0 \\ 0 & 0 & 0 & 0 & 0 & 0 & 1 & 1 & 0 & 0 & 0 & - & 0 \\ 0 & 0 & 0 & 0 & 0 & 1 & 0 & 1 & 0 & 0 & 0 & 0 & - \end{array} \right) & , \end{matrix} \quad (2.44)$$

where we left the values for self-interaction undefined (that is the $-$ in the matrix). And we will define the central frame format by indicating an ordered list of sites in the extended frame that have that format. In the example we are working, we will use $v_{cen} = [A_0, B_0, A_1, B_1]$.

2.5.1 Step 1: Finding all squares in the extended frame

Step one is to find all frames (not-permuted) that have the same format as the frame generated by v_{cen} . In order to implement that, we first generate the 4x4 adjacency matrix for the v_{cen} sites (using M_{ext}) and then we generate the matrices for all $4! = 24$ permutations. We keep the different generated matrices in a list Ψ_{cen} and the permutations that generate the same matrix as v_{cen} in a list L_{cen}^{sym} . This last list will have the permutations that do not change the relation between sites, meaning that it lists the symmetrical frames and it can be used to reduce the number of different blocks. For the example we are working on, there are just three different adjacency matrices formed by permutations of v_{cen} , these three form the Ψ_{cen} . In the list of matrix Ψ_{cen} below, the first one is the generated by v_{cen} , and the others are generated by the permutation in the line above the adjacency matrix, which is just one of the eight possible permutations of v_{cen}

² We name the sites a little differently in Appendix B, where we explain other approximations for the square lattice. The results are equivalent if you change $[E_1, E_2, E_3, E_4]$ to $[E_2, E_4, F_2, F_4]$.

³ In the cross approximation, which we will be making later, defining only the adjacency matrix will not suffice to characterize the relation between sites. Consequently, we will also define the 2-step walk matrix, and all tests made using the adjacency matrix will be equally made for the 2-step walk matrix.

that generates that same matrix:

$$\Psi_{cen} = \left\{ \begin{array}{c} \begin{pmatrix} A_0 & B_0 & A_1 & B_1 \\ - & 1 & 1 & 0 \\ 1 & - & 0 & 1 \\ 1 & 0 & - & 1 \\ 0 & 1 & 1 & - \end{pmatrix}, \begin{pmatrix} A_0 & B_1 & A_1 & B_0 \\ - & 0 & 1 & 1 \\ 0 & - & 1 & 1 \\ 1 & 1 & - & 0 \\ 1 & 1 & 0 & - \end{pmatrix}, \begin{pmatrix} A_0 & B_0 & B_1 & A_1 \\ - & 1 & 0 & 1 \\ 1 & - & 1 & 0 \\ 0 & 1 & - & 1 \\ 1 & 0 & 1 & - \end{pmatrix} \end{array} \right\}. \quad (2.45)$$

And there are eight symmetries in the square format, therefore there are eight permutations in L_{cen}^{sym} :

$$L_{cen}^{sym} = \left\{ \begin{array}{c} [A_0, B_0, A_1, B_1], [A_0, A_1, B_0, B_1], [A_1, B_1, A_0, B_0], [A_1, A_0, B_1, B_0], \\ [B_0, A_0, B_1, A_1], [B_0, B_1, A_0, A_1], [B_1, B_0, A_1, A_0], [B_1, A_1, B_0, A_0] \end{array} \right\}. \quad (2.46)$$

With this done, we can find which of the N_{cen} -combinations of all the $N = 12$ players generate a matrix equal to one of the matrices in Ψ_{cen} . In the cases in which the generated matrix matches one of the Ψ_{cen} matrices, we can find a permutation of that combination that matches the matrix generated from v_{cen} . This process identifies the square frames (non-permuted) in the extended frames. In the example, there are $\binom{12}{4} = 495$ combinations, and from these there are six square frames (non-permuted) in the extended frames:

$$\Phi_0 = \left\{ \begin{array}{c} [A_0, B_0, A_1, B_1], [A_0, B_0, A_3, B_3], [A_0, A_1, E_1, A_2], \\ [A_0, A_3, E_2, A_2], [B_0, B_1, E_4, B_2], [B_0, B_3, E_3, B_2] \end{array} \right\}. \quad (2.47)$$

Then $m_0 = 6$, and $c_0 = \{1, 1, 1, 1, 1, 1\}$. Where m_0 is the number of square frames found in the extended frame, and c_0 is the list of the exponents for the square block probabilities that will be multiplied to construct the approximation. In Figure 6, we visually represent the 6 frames that form Φ_0 , we can clearly see sites (and structures) appearing in more than one square, we will correct this ‘‘overrepresentation’’ in the next step (Step 2) by verifying how represented are each of the substructures of the square.

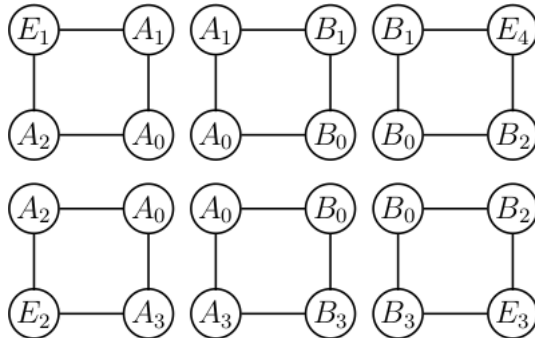


Figure 6 – Visual representation of the frames in Φ_0 .

2.5.2 Step 2 for R=1: Removing one site

When we remove one member from the square, we will always form the same subframe format: an L-format frame. Although there are differences in the generated adjacency matrix, these are only permuted cases of the same frame format.

$$\Psi_L = \left\{ \begin{array}{c} A_0 \ B_0 \ A_1 \quad B_0 \ A_0 \ A_1 \quad A_1 \ B_0 \ A_0 \\ \left(\begin{array}{ccc} - & 1 & 1 \\ 1 & - & 0 \\ 1 & 0 & - \end{array} \right), \left(\begin{array}{ccc} - & 1 & 0 \\ 1 & - & 1 \\ 0 & 1 & - \end{array} \right), \left(\begin{array}{ccc} - & 0 & 1 \\ 0 & - & 1 \\ 1 & 1 & - \end{array} \right) \end{array} \right\}; \quad (2.48)$$

There are in total $m_1 = 24$ L-frames in the extended frame, four for each of the six square frames in Φ_0 (we visually represent the L-frames in the square $[A_0, B_0, A_1, B_1]$ in Figure 7). They have no way of being repeated in two different squares (that are not permutations of each other) as there is no way for a square to share three vertices and not the fourth one with another square. All of them are represented in one, and only one, of the squares, resulting in $c_1[i] = 0 \ \forall i \in \Phi_1$. The effect of this is that we will not need to use the L-frames to calculate the probability for the extended frame.

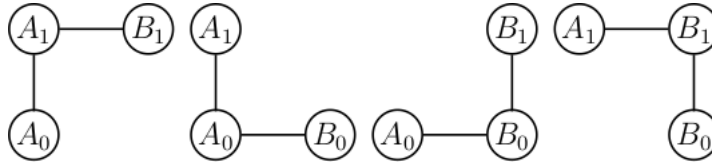


Figure 7 – Visual representation of the L-frames in the square $[A_0, B_0, A_1, B_1]$.

2.5.3 Step 2 for R=2: Removing two sites

By removing two sites from the square frame, we can generate two different frame formats: the pair and the diagonal-neighbour formats: $[A_0, B_0]$ and $[A_1, B_0]$ are, respectively, examples of these formats⁴. There are in total 17 pair frames (represented in Figure 8a) and 12 diagonal-neighbour frames, totaling $m_2 = 29$ frames in Φ_2 . In the same manner as for the L format, two squares frames can not share the same diagonal-neighbour without being a permutation of the same frame. Therefore, we will not use this frame in the extended probability. The same, however, does not happen to the pair frame, since $[A_0, B_0, A_1, B_1]$ and $[A_0, B_0, A_3, B_3]$ share $[A_0, B_0]$, for example.

⁴ Here again, for best characterization of the “diagonal-neighbour” format, we should use the two-step matrix, since the adjacency matrix for the two is null, but their relations lie in that they are the “diagonal” neighbours (different from very distant sites, for example, that have the same adjacency matrix). For simplicity, we will ignore this.

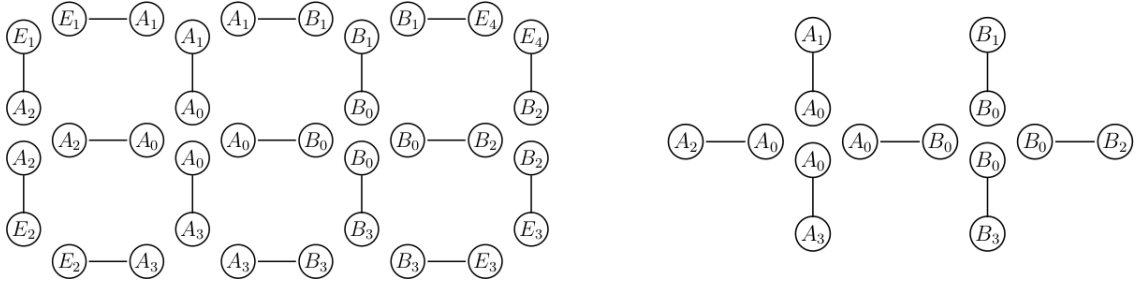
There are seven pair frames (represented in Figure 8b) that appear twice in the square frames, namely

$$\Phi_2\{[1, 7]\} = \{[A_0, B_0], [A_0, A_1], [A_0, A_2], [A_0, A_3], [B_0, B_1], [B_0, B_2], [B_0, B_3]\}, \quad (2.49)$$

while all other (size 2)-frames appear only once. Since $c_1[i] = 0 \forall i$, we do not have to consider how many times they appear in the L-frames. We can then write c_2 :

$$c_2[i] = \begin{cases} -1 & \text{if } i \in \Phi_2\{[1, 7]\} \\ 0 & \text{if } i \in \Phi_2\{[8, 29]\} \end{cases}. \quad (2.50)$$

The consequence of this step is that the approximation of $P_{3 \times 4}$ will be divided by the probability of the seven repeated pair blocks. In a way, we will be compensating for their overrepresentation in the square frames.



(a) All pair frames in the 3x4 extended frame. (b) The seven pairs ($\Phi_2\{[1, 7]\}$) that appear in two different square frames from Φ_0 .

Figure 8 – Pair frames in the 3x4 frame and repeated pair frames in Φ_0 .

2.5.4 Step 2 for R=3: Removing three sites

Finally, for the last case, we have $m_3 = 12$ different site frames in the extended frame. To obtain c_3 , we simple count the times they appear in the squares minus the times they appear in one of the seven pairs above:

Number of times in	A_0	B_0	A_1	A_3	A_2	B_1	B_3	B_2	E_1	E_2	E_3	E_4
Φ_0	4	4	2	2	2	2	2	2	1	1	1	1
$\Phi_2\{[1, 7]\}$	-4	-4	-1	-1	-1	-1	-1	-1	0	0	0	0
Total	0	0	1	1	1	1	1	1	1	1	1	1
c_3	1	1	0	0	0	0	0	0	0	0	0	0

(2.51)

This results in $c_3[A_0] = c_3[B_0] = 1$, while $c_3[i] = 0$ for $i \in (\Phi_3 - \{A_0, B_0\})$. The consequence of this step is that the approximation of $P_{3 \times 4}$ will be multiplied by the probability of the player strategies A_0 and B_0 . In a way, we will be compensating for their resulting underrepresentation in steps 1 and 2.

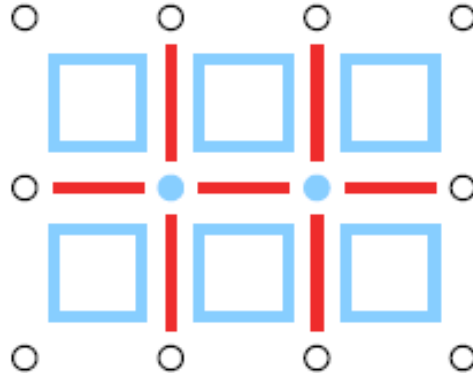


Figure 9 – Visual representation of the approximation for the 3×4 extended frame using squares. Light blue meaning that frame enters the approximation multiplying, while red means division.

2.5.5 Step 3: Writing the approximation for the extended frame

Now, we can finally write the approximation for the extended frame, resulting in:

$$P_{3 \times 4} = \frac{P_{\square}(A_0, B_0, A_1, B_1)P_{\square}(A_0, B_0, A_3, B_3)P_{\square}(A_0, A_1, E_1, A_2)P_{\square}(A_0, A_3, E_2, A_2)}{P_{-}(A_0, B_0)P_{-}(A_0, A_1)P_{-}(A_0, A_2)P_{-}(A_0, A_3)} \times \\ \times \frac{P_{\square}(B_0, B_1, E_4, B_2)P_{\square}(B_0, B_3, E_3, B_2)}{P_{-}(B_0, B_1)P_{-}(B_0, B_2)P_{-}(B_0, B_3)} P_{\circ}(A_0)P_{\circ}(B_0), \quad (2.52)$$

where we take the liberty of using A_0, B_0, \dots for the state of the A_0, B_0, \dots site, and we use closure conditions to obtain the pair probability P_{-} and the single site probability P_{\circ} for states S_0 and S_1 :

$$P_{-}(S_0, S_1) = \sum_{i,j} P_{\square}(S_0, S_1, i, j) = \sum_{i,j} P_{\square}(S_0, i, S_1, j) \quad \forall S_0, S_1; \quad (2.53)$$

$$P_{\circ}(S_0) = \sum_{i,j,k} P_{\square}(S_0, k, i, j) = \sum_k P_{-}(S_0, k) \quad \forall S_0. \quad (2.54)$$

We introduce a visual representation of equation (2.52) in Figure 9. Light blue meaning that frame enters the approximation multiplying, while red means division. In this way we can quickly and easily visualize an approximation, and rapidly check over and underrepresentation of structures. This use of a visual representation for the extension process was suggested in (SZABO; FATH, 2007, p. 207). The formula for $P_{3 \times 4}$ allows us to use it in equation (2.25) to calculate the evolution of the system for changes in the states of site A_0 and B_0 (the ones for which we can actually compute the ΔN function).

2.6 Reducing Computational Costs

The computational time increases based on the number of different configurations probed ($S^{N_{players}}$), which depends on the number of players in the extended frame ($N_{players}$) and the number of different strategies in the game (S). We will need bigger extended

frames for more precise approximations (considering larger structures and correlations between more distant sites). In latter sections, we will use extended frames with up to 18 players. In that case, for a game with 2 (3) strategies, there will be $2^{18} \approx 2.6 \times 10^5$ ($3^{18} \approx 3.9 \times 10^8$) different configurations.

Also, interpretation and readability of the data are another problem. For example, for a cross approximation (5-site) and a game with $S = 2$ strategies, there are $2^5 = 32$ different blocks in the central frame, meaning that there are $32 - 1$ different variables could be needed the state of the system. Using symmetries, we can reduce the number of variables in that case to $12 - 1$.

2.6.1 Symmetries

A great way to reduce the computational time is using a trick already used in section 2.2, when we considered that the probability for a pair CD and a pair DC is equal and that changes in CD and DC pairs could be counted together in $\Delta N'_{CD} \leftarrow \Delta N_{CD} + \Delta N_{DC}$. This trick works because the square lattice and the game⁵ are symmetrical under 180° rotations (also, for 90° degree rotations, and this is why we did not even consider using different probabilities for vertical and horizontal pairs). By using this fact, we reduce by half the number of states we had to sum over, since we only had to consider a CD pair in the center.

This concept can be extended both to other lattices with different symmetries as well as for higher order approximations, with the reduction in time being even greater. We can encounter the symmetrical blocks by identifying which permutations in the frame generate the same frame format. In the square example, in section 2.5, we could see that the following permutations of the frame $[A_0, B_0, A_1, B_1]$ generate the same frame format (in that case, the site relations are defined by the adjacency matrix):

$$L_{cen}^{sym} = \left\{ \begin{array}{cccc} [A_0, B_0, A_1, B_1], & [A_0, A_1, B_0, B_1], & [A_1, B_1, A_0, B_0], & [A_1, A_0, B_1, B_0], \\ [B_0, A_0, B_1, A_1], & [B_0, B_1, A_0, A_1], & [B_1, B_0, A_1, A_0], & [B_1, A_1, B_0, A_0] \end{array} \right\}. \quad (2.55)$$

If we apply these permutations to the state $CDCC$, for example, the four different states ($CDCC$, $DCCC$, $CCDC$, $CCCD$) will have the same probability. Applying to all different states, we can reduce the system, from the original 16, to 6 variables ($CCCC$, $CDCC$, $CDDC$, $CDCCD$, $CDDDD$, $DDDD$, as an example). For games with more strategies, the reduction is greater: $21/81 \approx 0.259$ for $S = 3$, and $55/256 \approx 0.21$ for $S = 4$.

⁵ As a counter example, a game where a D player has less probability to invade the left neighbour than the right one, even if their payoffs differences are the same, would break this symmetry

2.6.2 Inactive states

Another way to reduce the number of configurations probed is by determining which of the central blocks can be changed by the processes considered. For example, if the central pair in Figure 1.a was a CC pair, C players invading one another do not change the system. The same is valid for a DD pair. We can consider that the $CC(DD)$ pair is an “inactive” state, and ignore it in the summation, not even probing all different configurations around it. Another case occurs when there are players with fixed strategies that can not be copied or changed (for example, the hole in diluted lattices). It is obvious that pairs containing at least one such player are inactive states (considering no innovative process in the system). The cumulative effect of speed-ups gained by considering both symmetries and inactive states is presented in Table 2 for different cases.

Approximation	Strategies	2 (C, D)	3 (C, D, O)
	Pair		$1/4 = 0.25$
Square		$4/16 = 0.25$	$11/81 \approx 0.14$
Cross		$10/32 \approx 0.31$	$26/243 \approx 0.11$

Table 2 – Multiplicative effect on the number of configurations used in the approximation when considering both symmetries and inactive states for the case of 2 (C and D) strategies and 3 strategies (C, D , and a fixed O strategy) in the Pair, Square and Cross approximations for the square lattice.

2.7 Experimenting with different Extended Frames and Comparing Approximations

Since many different frames can be chosen to make an approximation for a certain central frame (pair, for example), we decided to test different extended frames and see the impact that these different approximations can have on the results.

To make this comparison we decided tested the same system as in Szabo & Toke (1998), which also makes MC simulations and pair, square and cross approximations for the system, without specifying the extended frame used. The system analysed consists of players positioned in a square lattice that play a weak PD with their first neighbours and with themselves (self-interaction). The changes are made by randomly choosing a pair of neighbours, and the probability of one player copying the other players’ strategy is given by a Fermi Transition function with $K = 0.1$ (see a detailed definition of the transition functions in Appendix D). We discuss if this system is really a weak Prisoner’s Dilemma or a snowdrift game due to the self-interaction in Appendix A.

We decided to make four approximations for the pair as central frame: the **Simple Pair** approximation which is usually made with unconnected neighbours of the central

pair, and is based on the approximation for a $4N$ Bethe lattice; the **Connected Pair** approximation, considering the eight-site frame needed to calculate the payoff of central players and their relations; the **Extended Pair** approximation which also considers what would be the diagonal neighbours of the central frame, forming a “ 3×4 ” rectangular frame; and **Second Neighbours Pair** approximation considering all the first and second neighbours of the central pair. In Figure 10, we represent visually these approximations. More details about each approximation are given in Appendix B, specially in Table 8.

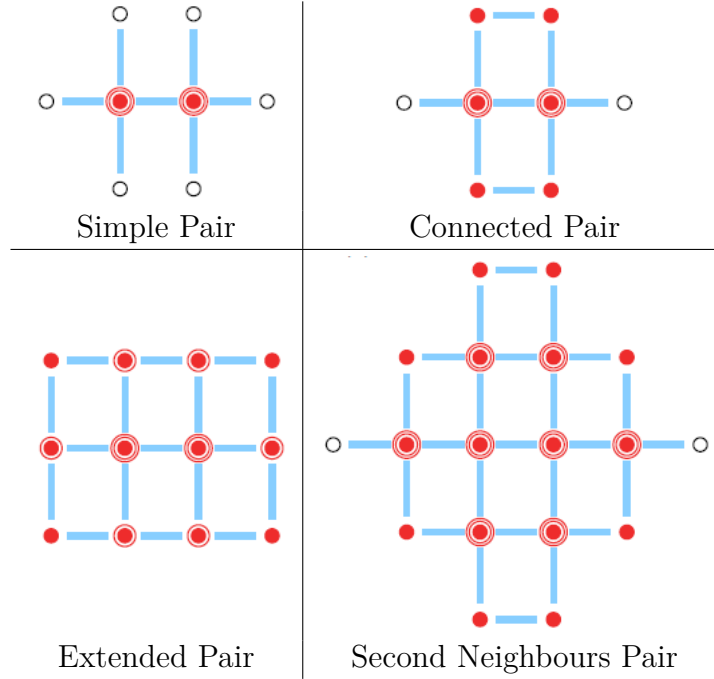


Figure 10 – Visual representation of the pair approximations being compared in Section 2.7.1. Light blue meaning the structure enters the approximation multiplying and red enters dividing, extra red circles around a site mean extra divisions. More detailed information in Appendix B, specially in Table 8.

We decided to make six approximations for the square as central frame: the **Reduced Square** approximation, in which we consider a square and its first neighbours (as shown below, this approximation causes a miscount in ΔN); the **4x4 Square** approximation, which, as the name indicates, utilizes an extended frame of 4×4 players; the **3x4 Square** approximation, where we consider invasions in the centralized pair only (sites A_0 and B_0 in the Appendix B); the **Mixed Square** approximation, where we consider a special neighbourhood and that only one player can be invaded (site A_0 being invaded by B_0 in the Appendix B). We detailed these approximations in Appendix B, specially in Table 9 where we present the visual representation of the approximation and its corresponding equation. We visually represent these four square approximations in Figure 11. Besides these four approximations, we also perform a test removing the step counting the representation of pairs and skip directly to counting the representation of points for the reduced square and 4×4 frame, generating two other approximations. This experi-

mentation serves to exemplify that using the more extensive correlations leads to better approximations.

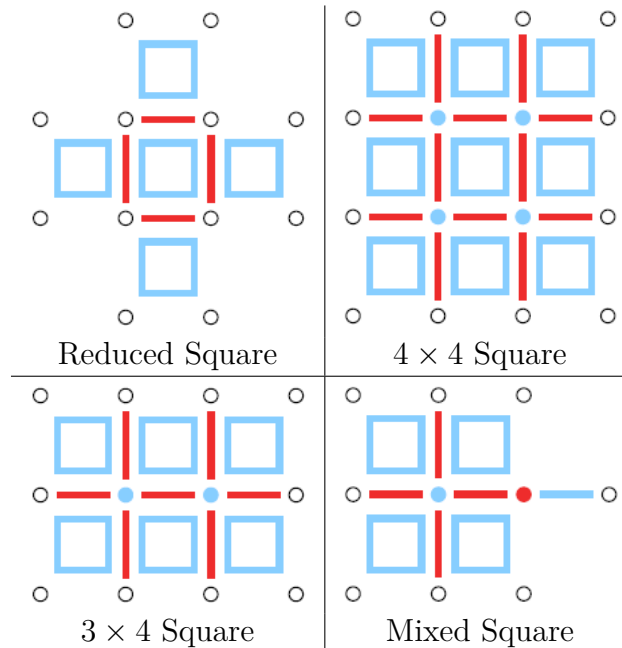


Figure 11 – Visual representation of the square approximations being compared in Section 2.7.2. Light blue meaning the structure enters the approximation multiplying and red enters dividing. More detailed information in Appendix B, specially in Table 9.

We decided to make three approximations for the cross: the **Minimal Cross** approximation, in which the extended frame contains basically a player and its first and second neighbours, only this player can change strategy; the **Double Cross** approximation, which considers all first and second neighbours of a pair of neighbours. We also used the Minimal Cross approximation with invasions of the first neighbours by the central player, which leads to ΔN miscounting in these processes. This exemplifies the importance of choosing an extended frame that allows a correct counting of ΔN .

As a method of checking which approximation is better for this system, we compare with the results obtained in Monte-Carlo simulations (averaged over 30 runs with randomized starting configuration for each value of temptation in a 100x100 square lattice). The results are shown in three different figures separating each according to the central frame of the approximation in Figures 13, 14, 15 for the pair, square and cross frame, respectively.

Visually, in Figure 13, the Connected Pair approximation curve seems to more closely resemble the MC curve, followed by the Second Neighbour Pair. The worst approximation seems to be the Simple Pair approximation. To better quantify this resemblance, we calculated the absolute difference between the result obtained with each approximation and the MC result, and present the (non-absolute) difference in Figure 13. We can see

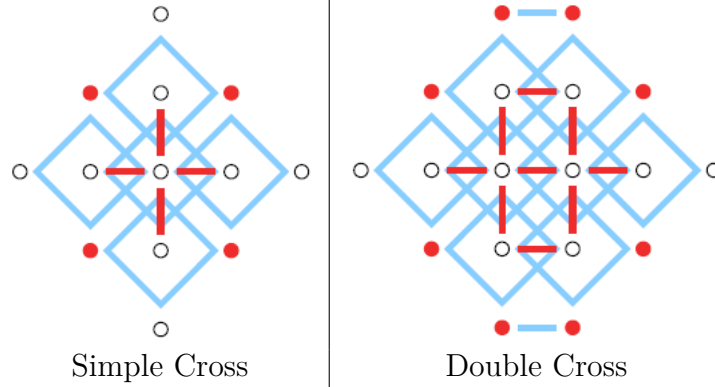


Figure 12 – Visual representation of the cross approximations being compared in Section 2.7.3. Light blue meaning the structure enters the approximation multiplying and red enters dividing. Rotated squares (diamond-shape) indicate the cross structures. More detailed information in Appendix B, specially in Table 10.

that the approximations differ the most from the MC result, around the transition points where the regime changes from coexistence to a single strategy dominating the system ($b \approx 1.22$ and $b \approx 1.85$). All curves reach a point where the difference is null, as they all cross the MC curve. We also plot the standard deviation of the MC average in order to show that the differences obtained are of a substantially larger order than the standard deviation, meaning that the difference is relevant.

We can also reduce this resemblance to a single measure, calculating the area under each of the absolute difference curves giving a measure of the total deviation. Although not shown in Figure 13, we extended this summation beyond $b = 2$, since the Extended and Simple Pair approximation still differ from the MC results in that range. Another interesting measure can be the maximum difference in a result, which is the measure of the maximum deviation from the MC curve. Besides that, we can see the difference in the critical temptation (b) for the regime to change from coexistence to single strategy dominance. That happens for $b_1^{MC} \approx 1.22$ and $b_2^{MC} \approx 1.85$. And we consider for this measure that the transition happens when one of the strategy probabilities drops below 5×10^{-4} . We present the results for these measures in Table 3, and analyse them in the following subsections.

2.7.1 Comparing Pair Approximations

As we can see in the comparison of all measures in Table 3 and visually in Figure 13, the Connected Pair approximation yields the best result amongst the pair approximations. The area measure is, respectively, almost 2 and almost 4 times smaller than the Extended and Simple pair approximations. Besides that, b_{crit} for the transition from coexistence to defection dominance is significantly better in the Connected Pair approximation, happening at a distance to the MC transition at least 10 times closer than the

Approximation	Total Area	Max diff	$b_1 (b_1 - b_1^{MC})$	$b_2 (b_2 - b_2^{MC})$
Monte Carlo average	–	–	1.22	1.85
Simple Mean-Field	0.481	1.000	1.00	
Simple Pair	0.171	0.244	1.04 (-0.18)	2.87 (1.02)
Connected Pair	0.041	0.154	1.04 (-0.18)	1.94 (0.09)
Extended Pair	0.075	0.183	1.02 (-0.2)	2.89 (1.04)
2nd neighbours Pair	0.052	0.183	1.02 (-0.2)	2.01 (0.16)
Reduced Square	0.084	0.327	1.34 (0.12)	1.91 (0.06)
4 × 4 Square	0.039	0.115	1.06 (-0.16)	1.86 (0.01)
Reduced Square (wp)	0.100	0.404	1.36 (0.14)	1.56 (-0.29)
4 × 4 Square (wp)	0.072	0.229	1.05 (-0.17)	1.58 (-0.27)
3 × 4 Square	0.038	0.115	1.06 (-0.16)	1.87 (0.02)
Mixed Square	0.046	0.123	1.06 (-0.16)	1.86 (0.01)
(ΔN wrong) Minimal Cross	0.141	0.314	1.32 (0.1)	1.96 (0.11)
Minimal Cross	0.013	0.068	1.11 (-0.11)	1.84 (-0.01)
Double Cross	0.011	0.076	1.13 (-0.09)	1.83 (-0.02)
Estimated error	$\pm 0.004^\dagger$	$\pm 0.015^\dagger$	$\pm 0.01 (\pm 0.02)$	$\pm 0.01 (\pm 0.02)$

Table 3 – This table presents four different measures for how much the different approximations resemble the MC results: Total area under the absolute difference curve between the approximation for temptation $b = [1, 3]$ (as presented in Figures 13, 14, 15); Max diff indicates maximum difference between the approximation and MC results; And the values of b_{crit} for both transitions between coexistence to single strategy domination (with the difference from the MC result in parenthesis). The best results among the different central frames are highlighted in a light blue shade and the best amongst all approximations are highlighted in a darker blue shade. In the first line, we present the Monte Carlo results obtained and, in the last line, we present estimates for the maximum measurement errors. [†] The value of estimated measure error for total area and maximum difference are the total area of the 1 sigma standard deviation curve for Monte Carlo simulations and the maximum standard deviation for Monte Carlo simulations, respectively.

other two approximations.

Comparing the Connected and Simple Pair approximations, it is expected that the Connected yields a better result than the Simple, as the latter approximation simply ignores some of the connections amongst players in that extended frame. Considering the correlations between the top (or bottom) line players significantly improves the approximation, without making it more computationally expensive. ⁶

Analysing those two approximations and the results obtained, we can expect that further increasing the extended frame, including more players and connections in the neighbourhood, would further improve the approximation, since this would add more

⁶ We are, of course, considering that the computational expenses scales with the number of different blocks/configurations we have to consider, and that the extra multiplications does not affect it much. Also, other implementations of the code could make the Simple Pair approximation much faster as discussed in section 2.6.

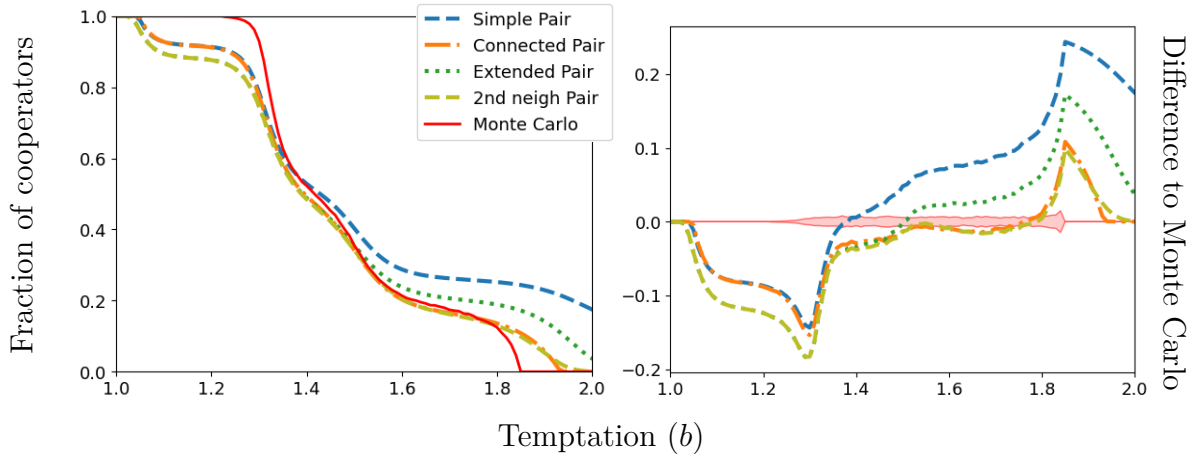


Figure 13 – Comparing pair approximations using different extended frames (Simple, Connected, Extended, Second Neighbourhood) with Monte Carlo results. The colored region in the second graph represents the one-sigma range (standard deviation of the sample) over 30 Monte-Carlo simulations for the system.

information about the first neighbours. Although this seems logical, comparing the results in Table 3 for the Connected, Extended and Second Neighbours Pair Approximation or analysing Figure 13, seems to contradict it. The 12-site rectangular neighbourhood and the neighbourhood including all second neighbours (18 players in total) pair approximations perform poorly compared to the Connected Pair (eight-site) approximation (but are still better than the Simple Pair), considering the increased computational costs due to the inclusion of more sites.

The “proposed lesson” we take comparing these approximations is that we should not overextend our frames, but still keep all essential information to the process under consideration. In this case, we should keep the information of the pair that has their payoffs compared and its first neighbours, so we can calculate those payoffs, and, of course, the information that some of those first neighbours are neighbours among themselves.

An interesting thing to notice is that Szabo & Toke (1998) used the Extended Pair approximation (the curves match exactly) referring to it as a “pair approximation”. However in other papers (HAUERT; SZABO, 2005; SZABO; FATH, 2007), where the authors explains the pair approximation in depth, they consider the Simple Pair approximation.

2.7.2 Comparing Square Approximations

We also decided to do some experimentation with different extended frames when using a square as central frame. We began testing two extended frames considering all invasions happening in the central square (all pairwise invasions in that square). The first frame considered was the central square and their first neighbours, totaling 12 sites (we call this the Reduced Square approximation). We also built a second extended frame with a grid of 4×4 players (that is the same frame as the first one plus the four sites that

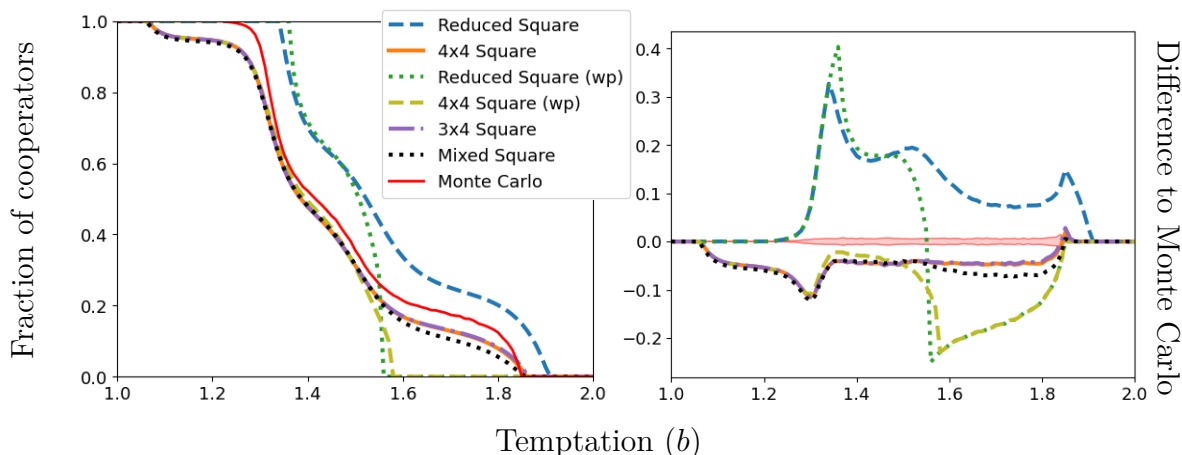


Figure 14 – Comparing square approximations using different extended frames: Reduced, 4×4 , 3×4 , Mixed, and testing some cases omitting pair division marked with (wp), with Monte Carlo results. The colored region in the second graph represents the one-sigma range (standard deviation of the sample) over 30 Monte-Carlo simulations for the system.

are in the corners, and we call this the 4×4 Square approximation). The first one has a problem: when one of the sites in the central frame is updated, not all square frames with that site which are in the lattice are also in this extended frame. An example, looking at the visual representation of the Reduced Square in Table 9 in the Appendix B, would be that when we change the player in the second line and second column (A_1), the square in the top left corner (formed by A_1 , E_1 , G_1 , E_2) is not present as it is in the second extended frame considered. This makes our counting function ΔN deviate from its true value, since we do not count changes in the missing square.⁷ Comparing the results in Table 3 and visually in Figure 14, we can see that this deviation makes the approximation perform quite poorly, being outperformed even by the pair approximations (unless when predicting the first and second transition points).

We also decided to experiment with a different approximation: when building the approximation for those extended frames, we did not divide by pair probabilities, going straight to the site probabilities for “correcting overrepresented” players. This was tested as this could simplify the automated extension process, reducing the steps to implement it. The result for these changes can be seen in Table 3 and in Figure 14 marked with (wp); they exemplify the importance of correctly applying the automated extension process, as the performance of these approximations without pair division is far worse than the ones with it, for the same extended frame. It is also interesting that, in both cases, the removal of the pair probability division leads to a far earlier transition from coexistence to defector dominance, without a significant change in the transition point of cooperator dominance

⁷ We can try to correct ΔN with estimations of what that missing square could be, but this was not implemented as this would make ΔN dependent on the probability values of blocks, and not only on the process taking place and configuration. In a certain way, we would be transferring part of the probability of the extended frame to the ΔN function.

to coexistence.

Using the concept from the pairs that we should not overextend our extended frame, we decided to test a third and fourth frames. The difference being that, in this case, we would not use all processes occurring in a square (which is our central frame in this approximation). We built our extended frame from the basic pairwise interaction and their first neighbours only including other players if they would make us err in the same way that the Reduced Square errs, that is miscounting ΔN . This leads to what we called the 3×4 Square (12-site) and the Mixed Square (10-site) approximations. The 10-site approximation has the peculiarities that the invaded player must be the left one from the central pair as explained in Table 9 (in Appendix B). Besides that, there are pair and site probabilities both in the numerator and denominator in the approximation. The 3×4 Square performs as well as the 4×4 Square approximation, and the curves almost match each other, but with the advantage that there are only $1/2^4 = 1/16$ of the blocks compared to the 4×4 approximation. The Mixed Square performs quite well, but has a worse result than the 3×4 Square. We could improve it by introducing the use of L-frame format probabilities, which we did not test. The computational cost does not decrease much from the 3×4 Square due to the broken symmetry not allowing us to use some of the speed up tricks used in the other approximations, although the number of sites is reduced.

2.7.3 Comparing Cross Approximations

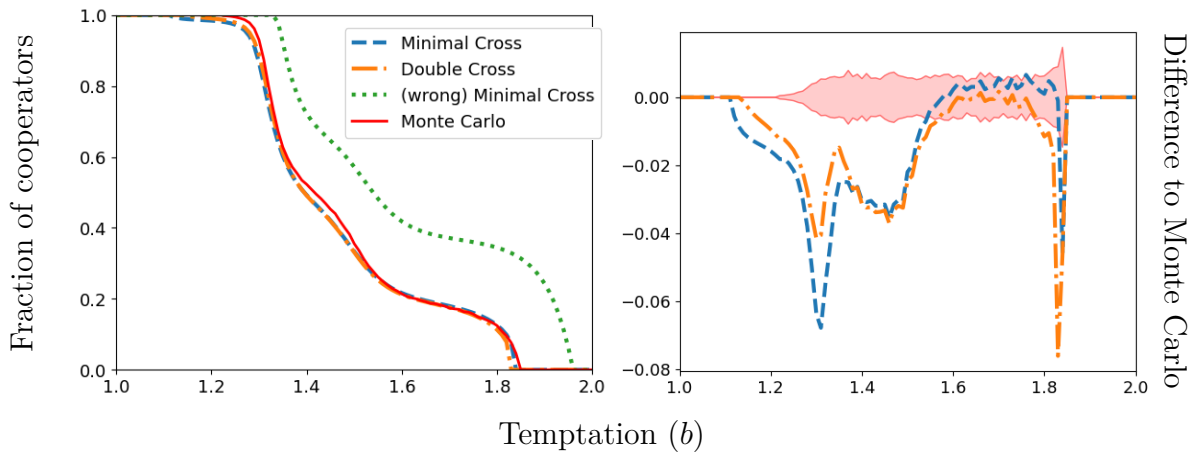


Figure 15 – Comparing cross approximations using two different extended frames (and an extra one which miscounts ΔN , marked as “(wrong) Minimal Cross”) with Monte Carlo results. We don’t present the “(wrong) Minimal Cross” in the difference to MC, as they would make it harder to visualize the difference between the other two approximations. The colored region in the second graph represents the one-sigma range (standard deviation of the sample) over 30 Monte-Carlo simulations for the system.

We also tested using a cross as the central frame, which consists of a player and

its four neighbours in the lattice and built two extended frames. In the first, we added all of the central player's first and second neighbours to the extended frame (allowing us to correctly calculate ΔN for the case in which the central player changes state), in a total of 13 sites in the frame, calling it the Minimal Cross frame. In the second, we consider a pair and include all first and second neighbours of this pair, allowing us to correctly calculate ΔN for both players in the pair. This frame includes 18-sites and we call it the Double Cross frame. The ideas for building the frames centered on a player (Minimal Cross) or a pair (Double Cross) are the same as the ones used in building the Mixed Square and the 3×4 Square frames, respectively.

Looking at Figure 15, we can see that Minimal Cross and Double Cross are quite close to each other. Considering its measurements in Table 3, we can see that all differences in the measurements are within the estimated maximum error. That means that the two approximations perform quite similarly. Using the square cases as comparison, we would expect that the Double Cross should outperform the Minimal Cross (in the same way the 3×4 Square outperforms the Mixed), which can be seen in some measurement, but those differences are not significant. The difference in computational costs between these two approximations is significant, because we have $2^5 = 32$ times more configurations in the Double Cross frame for this system.

To more firmly stress that a ΔN miscalculation introduces an error in the Reduced Square case, we implemented the Minimal Cross evolution in two ways: one in which we considered that the central player can invade and be invaded by its neighbours; and another where only the central player can be invaded. In the first, the ΔN function will be miscounted for the neighbours, since not all cross frames in the lattice they are part of are in this extended frame. The second will not have this problem, because only the central player will be invaded, and ΔN can be correctly computed using this extended frame. In Table 3 and Figure 15, we present the results for the first evolution as “(ΔN wrong) Minimal Cross”, and, for the second, simply as “Minimal Cross”. From the measurements, it is obvious that the one with the wrong ΔN computation has a poorer performance across all measurements. Also, by looking at Figure 15 (or measurements of b_1 and b_2), it favors cooperation by dislocating both transitions to higher values of b .

2.7.4 Guiding Principles for choosing the extended frame

By analysing the results, we create a “guiding principle list” for choosing the extended frame for the approximation:

1. It, obviously, must allow us to calculate the probability for the process to happen. In our example, we needed a pair and its first neighbours, allowing us to calculate the payoff difference for the pair.

2. It must allow us to correctly compute the ΔN function for the sites we intend to be updatable, and, for that, we must include all central frames in the lattice to which the player changing states belongs.

2.1 (optional) It must also allow us to correctly calculate ΔN function for the player being copied as this may, or may not, improve the approximation. The case tested are within our error margin, so we can not conclude either way.

3. It must not “overextend”, which means it must not include more players than those necessary to fulfill the items above, as this generally does not improve, and can even impair the quality of the approximation at an increased computational cost.

3 Applications to Diluted Lattices

As exposed in chapter 1, there are some cases in which diluting a lattice may be beneficial to cooperators (VAINSTEIN; ARENZON, 2001). In this chapter, we use local approximations as explained in section 2.4 to explore the mechanisms under this increase of cooperation. We specially use the Connected Pair approximation (detailed in Appendix B) to analyse the behaviour in the diluted square lattice and we develop other pair approximations for other lattices: Honeycomb; Cubic; Triangular; Bethe trees with 3, 4, 5, 6 neighbours.

As it was noted by Wang, Szolnoki & Perc (2012a), the analysis of weak PD and Snowdrift games with a Fermi transition function in the Square ($K = 0.4$), Honeycomb ($K = 0.3$), Cubic ($K = 0.6$) and Triangular ($K = 0.6$) lattices indicates that the percolation threshold may have a particular importance to this mechanism of enhancement of cooperation:

More importantly, if b is close to the critical value at which cooperators would normally die out, the optimal population density is strongly related to the percolation threshold of the interaction graph ... Accordingly, percolation plays a key role by the resolution of social dilemmas by significantly elevating the effectiveness of spatial reciprocity. (WANG; SZOLNOKI; PERC, 2012a, p. 2)

Further investigations of the weak PD in a diluted square lattice done by Leivas (2018) shows that the breaking of the lattice into multiple independent clusters is also important. With Cooperators having a better survival chance in larger clusters (bigger than 100 sites) than in smaller ones. Besides that, Leivas (2018) shows that a replicator transition function can reproduce the peak of cooperation close to the percolation threshold if a perturbation is added.

Another investigation, in the same analytical vein as the present work, by Xu et al. (2016), considers the snowdrift game using a replicator transition function (with payoff normalized by the number of neighbours) on a square lattice and they point out the importance of local payoff levels and the redistribution of players among different payoff levels due to dilution leading to increase in cooperation. Xu et al. (2016) considers that the pair approximations do not show the qualitative behaviour of the peak of cooperation: “*For the bigger clusters, we show that the pair approximation is inadequate. This inadequacy points to the necessity of incorporating a longer spatial correlation in to the theory*”. Their model of pair approximation differs from ours as there is no strategy-hole correlation in theirs. In our analysis, the evolution of different correlations between cooperators and defectors with holes is an important feature of the system. This may be the

reason why their pair approximation fails to capture the peak of cooperation while a cross approximation (which has player-hole correlations included) captures it. Our pair approximations capturing the qualitative behaviour of the system indicates the relevance of the local structure and the importance of the levels of transition in the transition function ω for the appearance of the cooperation peak.

3.1 Approximations for the Diluted Lattice

In our model, we chose to consider a diluted lattice not as a different lattice from the original, but rather we suppose that the game has changed: now besides the players playing either cooperation (C) or defection (D), there are a fixed number of players with a new strategy O that can not be copied or changed, and it gives zero payoff when playing both with cooperators and defectors. Indeed, these O players can be seen as the holes in a diluted lattice. This allows us to use one extended frame instead of multiple extended frames with different probabilities, as was done by Xu et al. (2016). And since O is regarded as a strategy, we can see C or D players developing different probabilities of being near the holes, as this is quantified as one of the probabilities.

The weak Prisoner's Dilemma is represented by the following payoff matrix with the addition of the O strategy:

		Player Y		
		C	D	O
Player X	C	1	0	0
	D	0	0	0
	O	0	0	0

Table 4 – Payoff for the weak Prisoner's Dilemma adding an O fixed strategy to represent unoccupied sites. Since the payoff for the hole is not used in any calculation, we mark it with an asterisk (*).

Analysing the system in this way, we can also question whether the zero payoff could influence the phenomenon. Maybe holes giving (or subtracting) a different payoff can change the system's behaviour. This payoff given by a hole could be explained in many ways. For example, it could be that the absence of a player in that region results in an abundance of resources that can be explored by the neighbours, or it could represent the opposite scenario. Testing whether this changes the system behaviour would be interesting. In our model, the payoff given by the hole to a cooperator or a defector is the same as a defector gives them: zero. This invites us to do a comparison: of a hole being a unchangeable and uncopyable defector. This comparison fails in the case of the Snowdrift

game, as tested in Wang, Szolnoki & Perc (2012a), although the payoff given by the hole still matches the lowest payoff in this game, that of $P = 0$, and in this case the cooperation peak still appears. Interestingly, in this same paper, it is shown that for the Stag-Hunt model, in which the lowest payoff for an interaction is $S = -r$ and thus lower than the payoff given by holes, the cooperation peak is not reproduced. Another way this comparison can be broken is in the system analysed by Xu et al. (2016), where the players have their payoff divided by the number of players around them before comparison. In this way, the holes give a small boost to players surrounded by them based on their performance with other players. This does not appear to change the behaviour of the system and addresses some questions raised in Szolnoki, Perc & Danku (2008), in which, for some scale free networks, normalizing by the different number of neighbours makes the benefit to cooperation decrease. Although we raise this question of the zero payoff of holes, we do not pursue it.

Also, the choice of considering a hole as a strategy facilitates the application of other approximations and the development of the differential equations. As it is pointed out by Xu et al. (2016), considering different extended frames and its different probabilities for the holes is a complicated task:

... we propose a site-diluted evolutionary snowdrift game and focus on studying the effects of disorder. Although there were similar simulation results reported in disordered models using different evolutionary mechanisms, our focus is to present a theoretical framework that can be applied to a wide range of problems concerning competing games in disordered systems. This is a challenging task as theoretical analysis of evolutionary games in regular lattices is far from satisfactory, let alone disordered lattices. (XU et al., 2016, p. 2)

When performing a pair approximation with these three strategies, compared to the example in section 2.2, we will not only have the probabilities $P(C, C)$, $P(C, D)$, $P(D, D)$, but also the probabilities $P(C, O)$, $P(D, O)$, $P(O, O)$. Due to the fixed amount of holes, the probabilities will have the following relations with the site occupancy parameter ρ :

$$P(O, O) = (1 - \rho)^2 \quad (3.1)$$

$$P(C, O) + P(D, O) = \rho(1 - \rho) \quad (3.2)$$

$$P(C, C) + 2P(C, D) + P(D, D) = \rho^2 \quad (3.3)$$

We know that the probability of one hole being next to the other ($P(O, O)$) is fixed as shown in equation (3.1), and by equation (3.2) we know that $\dot{P}(C, O) + \dot{P}(D, O) = 0$, as ρ is a constant of the system. Therefore, the system state can be defined by three independent variables (as an example: $P(C, C)$, $P(C, D)$, $P(C, O)$), needing only one extra independent variable when compared to the pair approximation for the undiluted lattice.

For the square lattice analysis, we decided to use the Connected Pair approximation, which we argued in section 2.7.1 to be the best pair approximation. The details of this approximation can be seen in Table 8, in Appendix B. For the other lattices, we developed different pair approximations, presented in Appendix C.

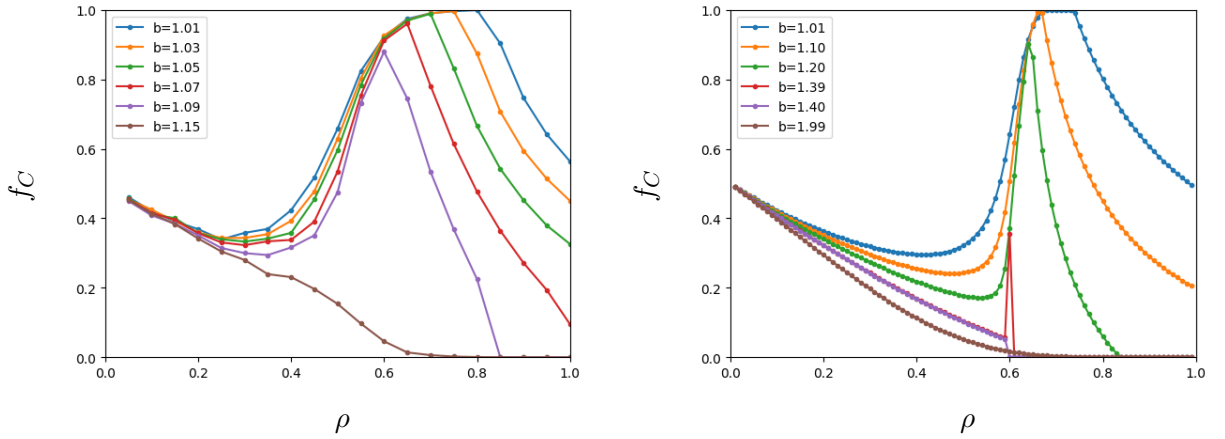
3.2 Results for the Diluted Square Lattice

We will start analysing the same system as given by Wang, Szolnoki & Perc (2012a): a weak PD in a diluted square lattice with a Fermi transition function with $K = 0.4$. We compare the fraction of cooperators $f_C = P(C)/\rho$ (that is the fraction of non-hole players that are cooperators) obtained by MC simulations in Figure 16a with those obtained from the Connected Pair approximation for the square lattice in Figure 16b. We notice that the behaviour of the system is only captured in its qualitative way by the approximation, without numerical precision.

Comparing the graphs in Figure 16, we can see that this pair approximation presents similar cooperation peaks for intermediate values of ρ . And most interestingly, this peak disappears for b increasing around the same value of $\rho_* \approx 0.6$, which is close to the site percolation threshold $\rho_{crit} \approx 0.59$. We can see that for $b = 1.01$, the curve is similar, but in the pair approximation there is a complete extinction of defectors for a range of values of ρ around $\rho = 0.7$. For other values of b , this pair approximation fails in its predictions of which b values presents these peaks, allowing the presence of it until $b_{max} = 1.39$, a far higher value than $b_{max} \approx 1.09$ obtained in MC simulations. This could be expected as this approximations favours the cooperators even in a undiluted lattice, as we can see by the existence of cooperators at $\rho = 1$ and $b = 1.1$, while in MC simulations for a full lattice the cooperation is extinct by $b \approx 1.07$ (SZABO; FATH, 2007, p. 157).

Interestingly, in the approximation for $b = 1.4$ and other values beyond, there is a gap around $\rho = 0.6$, with cooperators discontinuously jumping from complete absence to coexistence (with f_C substantially larger than zero). This gap closes, and then disappears, with increasing b . This is interesting for two reasons. First, because we know there are almost 2.6% of isolated players at the lattice for $\rho = 0.6$ and, in the pair approximation, the half of those which start as cooperators get extinguished even being completely isolated for $b = 1.4$ but not for some higher b (e.g. $b = 1.99$ in Figure 16b). This is probably linked to the different speeds of process happening: for low b , the invasion of defectors is slow enough that the mixing of pairs do not separate the population before extinction, while at high b this separation occurs. The second reason is that this could indicate that the $\rho = 0.6$ seems to be important as a transition point for what is happening locally, not only in the larger structure.

We decided to continue using the Connected Pair approximation to explore this

(a) According to the Monte Carlo simulations in a 100×100 lattice.

(b) According to the Connected Pair approximation.

Figure 16 – Values of the fraction of cooperators (f_C), given a site occupancy ρ , for a diluted square lattice, transition function ω is Fermi with $K = 0.4$. Different curves for different values of b .

system under different transition functions ω (the details of one are presented in Appendix D): Heaviside, Replicator, and Fermi with $K = 0.01$, with $K = 0.1$, with $K = 1.00$. The results are presented in Figure 17, with the cooperators' fraction f_C represented in color-scale for different values of parameters ρ and b .

What we can see in Figure 17a is that with the Heaviside transition function, the peak of cooperation appears at $\rho_* = 0.72$ and ceases when $b > 1.5$. For increasing values of K in the Fermi transition function (remember that for $K \rightarrow 0$ the Fermi becomes a Heaviside), we can see in Figures 17b to 17e, that the peak for cooperation starts to cover a region of values of ρ for lower b and is dislocated for lower values of ρ for higher b ; we obtain a peak close to the $\rho_{crit} \approx 0.59$ for $K = 0.4$ ($\rho_* = 0.6$), the same as used in Wang, Szolnoki & Perc (2012a). However, it keeps moving to lower values with further increases of K and for $K = 1.0$ it reaches $\rho_* = 0.52$. Further investigation is needed as to whether this also happens in MC simulations. In Figure 17f, we can see that the replicator has the strangest behaviour: for increasing b , the peak moves in the opposite direction for increasing ρ . Not only that but the fraction of cooperators may increase when increasing b for some fixed values of ρ . We believe, again, this is due to the sensibility to the speed for different processes to happen, and in the replicator function these speeds vary drastically.

To better visualize this displacement of the cooperation peak, in Figure 18 we compare ρ_{max} , where the (local) maximum in the fraction of cooperators happens, for each b and for each different transition function. We note that due to the extinction of defectors (that is when the fraction of cooperator reaches 1), in some cases, ρ_{max} comprises a range of ρ values.

To better understand what is happening in the pair approximation, we analyse

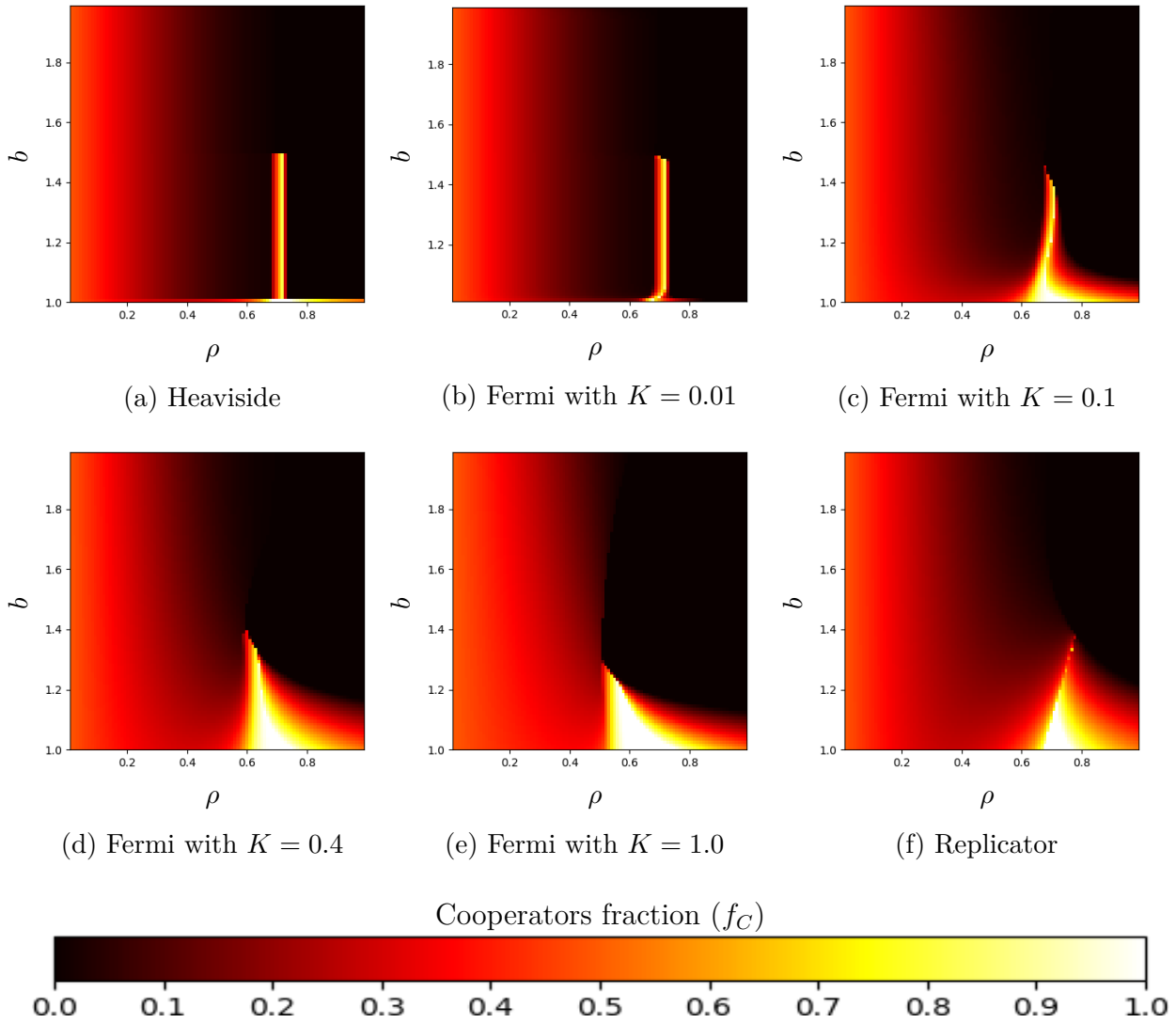


Figure 17 – Prisoner’s Weak Dilemma in a diluted Square Lattice obtained with the connected pair approximation. In the x-axis, we have the density (ρ) of players and in the y-axis, Temptation (b) and in color scale we can see the fraction of not-holes that are cooperators.

the final state for the case of the Heaviside for $1 < b < 1.5$ and $\rho = 0.72$ (where the maximum of cooperation happens). The final state of the system is $P(C) = 0.587$ ($f_C = 0.815$), $P(D) = 0.133$. In more detail we can see the pair probabilities $P(CC) = 0.437651$, $P(CD) = 0.000001$, $P(DD) = 0.080746$, $P(DO) = 0.051798$, $P(CO) = 0.149802$. Two interesting things can be seen: that $P(CD) \rightarrow 0$, which means that the frontier between the C and D almost disappears, being separated by O players; and $P(DO) - P(D)P(O) \approx 0.0146$ (or, to better exemplify $\frac{P(DO)}{P(D)P(O)} \approx 1.39$), that means during this separation it seems that the defectors are more likely to get stuck with holes around them than other players. Actually $P(DO) - P(D)P(O)$ generally also has a peak together with the peak of cooperation. These two behaviours can be seen across all transition functions around the maximum of the cooperators’ fraction.

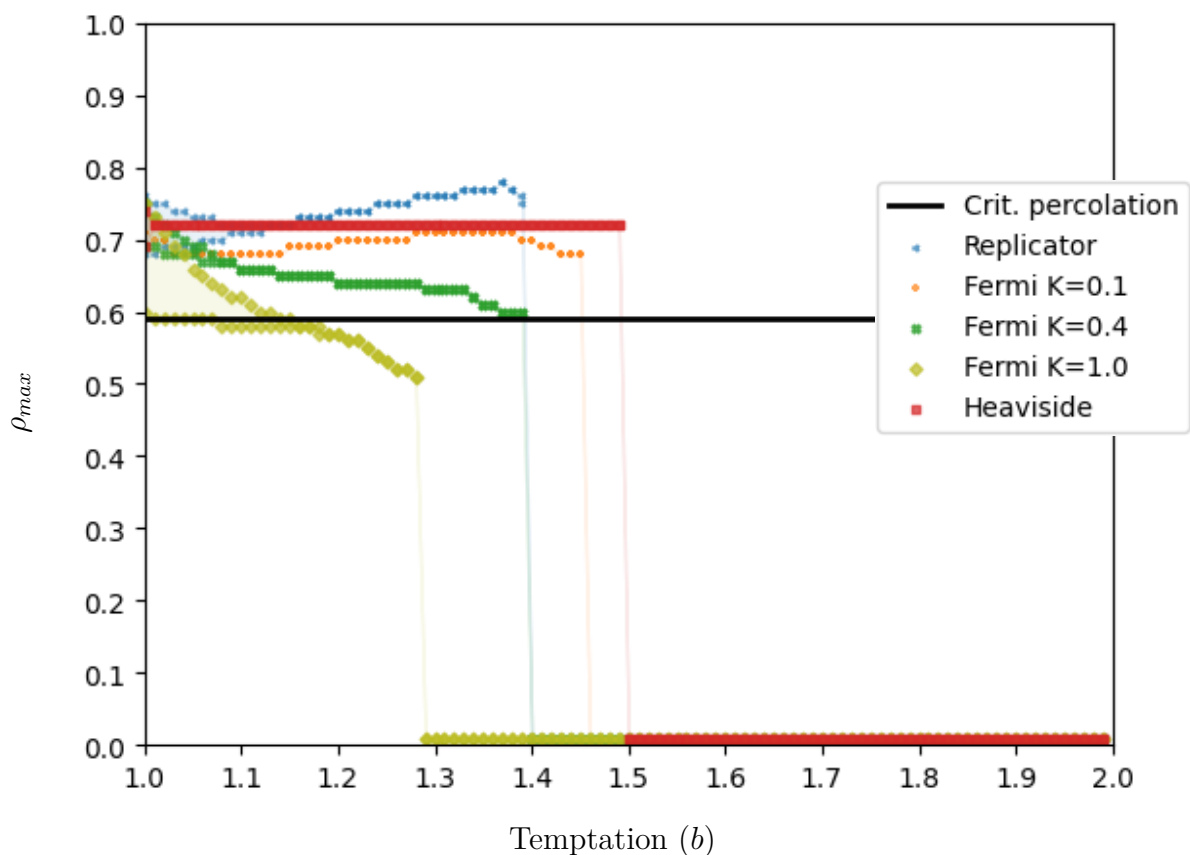


Figure 18 – Square lattice ρ_{max} comparison for different ω transition functions, according to the Connected Pair approximation.

3.2.1 Possible explanation for the diluted square lattice

We can try to understand the behaviour of the pair approximation by looking at the probability of a player having N occupied neighbours ($P(N, \rho)$), which can be easily calculated by:

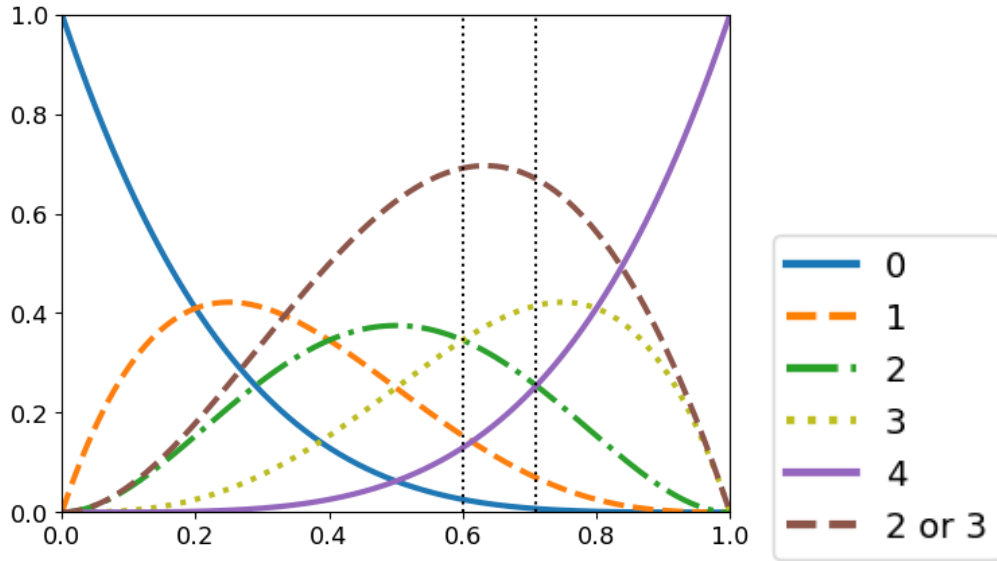
$$P(N, \rho) = \binom{4}{N} \rho^N (1 - \rho)^{4-N}, \quad \text{for } 0 \leq N \leq 4; \quad (3.4)$$

and the probability of a pair having N and M neighbours ($P(N, M, \rho)$), which can be calculated by:

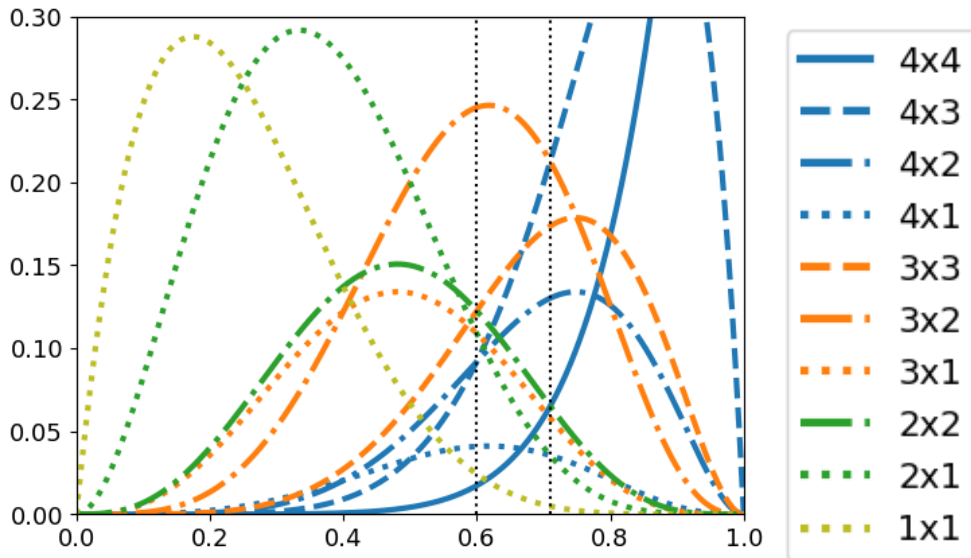
$$P(N, M, \rho) = \frac{P(N, \rho)P(M, \rho)}{1 - P(0, \rho)}, \quad \text{for } 0 < N, M \leq 4. \quad (3.5)$$

We show the different $P(N, \rho)$ in Figure 19a, where we can see that for $\rho = 0.6$, the probability of having 2 and the probability of having 3 neighbours is the same. Also, another transition happens close to this value (actually, at $\rho \approx 0.614$): when it becomes more probable that players have 4 neighbours than 1 neighbour. Also around $\rho \approx 0.71$ is the point where players have the same probability of having 3 or 4 neighbours. These points $\rho = 0.6$ and $\rho \approx 0.71$ are also important transitions in the probability of a pair

of neighbours having N and M neighbours, as it can be seen in Figure 19b, because $P(N, M, \rho)$ is basically $P(N, \rho)$ multiplied by $P(M, \rho)$ with a normalization.



(a) Probability a player has N neighbours for changing ρ parameter. We also plot the probability of a player having 2 or 3 neighbours, that is $P(2, \rho) + P(3, \rho)$.



(b) Probability a pair having N and M neighbours for changing ρ parameter. Here we summed the probability of pairs having 2, 3 neighbours with 3, 2 neighbours, so for $N \neq M$ we double $P(N, M, \rho)$ to define the probability of having 2*3 neighbours, for example.

Figure 19 – Probabilities for the local structures for a player and a pair.

The probability of a pair of neighbours having N and M neighbours is an important quantity to understand the possible (and most probable) local payoff configurations. We present in Table 5, for $b = 1.05$, the probability of the $D \rightarrow C$ process (Defector invading a Cooperator) minus the probability of the $C \rightarrow D$, when the C has n_C cooperator neighbours and the D has n_D cooperator neighbours.

A possible explanation is that, in the case of a Heaviside transition function, the

Cooperation enhancement at $\rho = 0.72$ is due to the most common local configuration being a player with 4 neighbours playing against one player with 3 or 2 neighbours (or even 1 neighbour). Thus, according to Table 5a, if the Cooperator occupies the place with four neighbours and is surrounded by other cooperators (the evolution generally leads to $p(CC) > p(C)p(C)$), it can invade the defector. This mechanism works, but when lowering ρ the probability of having four neighbours decreases, so the cooperators lose its advantage. We can see that when $b > 1.5$, the peak does not appear, that is when there is a change in Table 5a, for $n_D, n_C = 2, 3$ from -1 to 1 , and cooperators are invaded any time they have their payoff compared with a defector has at least one other cooperator neighbour.

		n_C			
		0	1	2	3
n_D	1	1	1	-1	-1
	2	1	1	1	-1
	3	1	1	1	1
	4	1	1	1	1

		n_C			
		0	1	2	3
n_D	1	0.8649	0.0624	-0.8298	-0.9848
	2	0.9896	0.8798	0.1244	-0.8093
	3	0.9992	0.9908	0.8932	0.1853
	4	0.9999	0.9993	0.9919	0.9051

		n_C			
		0	1	2	3
n_D	1	0.9253	0.3584	-0.7039	-0.9719
	2	0.9970	0.9640	0.6351	-0.4621
	3	0.9999	0.9986	0.9828	0.8093
	4	1.0000	0.9999	0.9993	0.9919

(a) Heaviside, for values of $1 < b < 1.5$. (b) Fermi with $K = 0.4$, $b = 1.05$. (c) Fermi with $K = 0.4$, $b = 1.30$.

Table 5 – Tables presenting the values of $\omega_{D \rightarrow C} - \omega_{C \rightarrow D}$ for different configurations of number of cooperator neighbours of the cooperator (n_C) and of the defector (n_D) for two different transition functions. We can obtain $\omega_{D \rightarrow C}$ ($\omega_{C \rightarrow D}$) from any of the values displayed on the table, x , as $\omega_{D \rightarrow C} = \frac{1+x}{2}$ ($\omega_{C \rightarrow D} = \frac{1-x}{2}$).

Now, analysing Table 5b, we see that for $b = 1.05$, the change from a Heaviside to a Fermi transition with $K = 0.4$ can not be considered a small perturbation in the system. In this case, a cooperator playing against a defector with the same total number of cooperator neighbours has a 40% to almost 50% chance of invading the defector, while for other configurations the player which has more chance to invade has at least a 10 times higher probability of doing so than of being invaded ($|\omega_{D \rightarrow C} - \omega_{C \rightarrow D}| > 0.81$ implies that $\max\{\frac{\omega_{D \rightarrow C}}{\omega_{C \rightarrow D}}, \frac{\omega_{C \rightarrow D}}{\omega_{D \rightarrow C}}\} > 10$). This almost 50% chance of invading a defector greatly benefits cooperators, since when it invades, it strengthens the position of the original cooperator, while if the defector is the one invading, it weakens the position of the original defector (which will still have cooperator neighbours to fight against). This could be measured in the ΔN for these processes in these different configurations.

We can see in Figure 18 that the peak for $b = 1.05$ happens for a range of values of ρ around 0.7, since cooperators have an advantage when it has 4 neighbours, as well as when it has 3 or 2, so we see this peak of cooperation spread for a range of ρ . Increasing b to $b = 1.3$, we can see in Table 5c, that having 4 neighbours is not as advantageous as before, but having 2 or 3 neighbours still be enough, if your neighbours have less neighbours than you, hence the peak moves to values close to $\rho = 0.6$, where this happens and having 4 neighbours is less probable.

3.3 Prisoner's Dilemma in other lattices

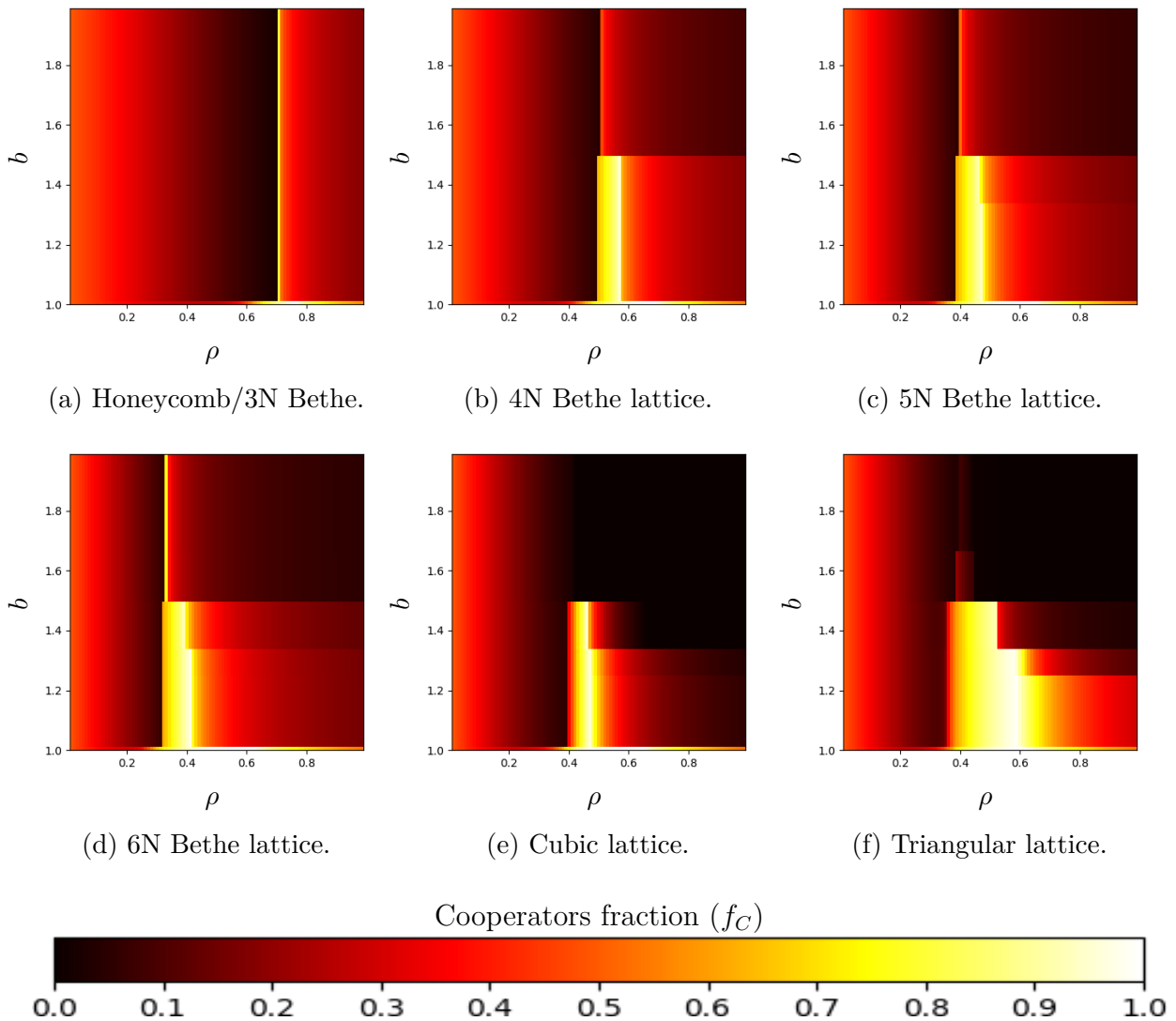


Figure 20 – Results obtained from pair approximations for a Weak PD in different diluted lattices using a Heaviside transition function (detailed in Appendix D). In the x-axis, we have the density (ρ) of players and in the y-axis, Temptation (b) and in color scale we can see the fraction of occupied sites that are cooperators (f_C).

We also investigated other lattices using a Heaviside transition function. Besides the Triangular, Cubic and Honeycomb, we studied Bethe trees with 3 to 6 neighbours. The details for the pair approximations used are in Appendix C. The 3N Bethe pair approximation is not different from the approximation made for the Honeycomb lattice. The 4N Bethe tree pair approximation is equivalent to a Simple Pair approximation for the square lattice. So, we can compare these two approximations for the square lattice again. In the same way, the 6N Bethe lattice pair approximation can be seen as an approximation for the cubic lattice where we disregard the relations among the sites around the central pair.

The results for these lattices are shown in Figure 20. We again see that we are able to replicate the appearance of a peak of cooperation for middle values of the site occupancy ρ . The two behaviours pointed out in the square lattice ($P(CD) \rightarrow 0$ and $P(DO) \gg P(D)P(O)$) also happens in each of these lattices when close to the cooperation peak.

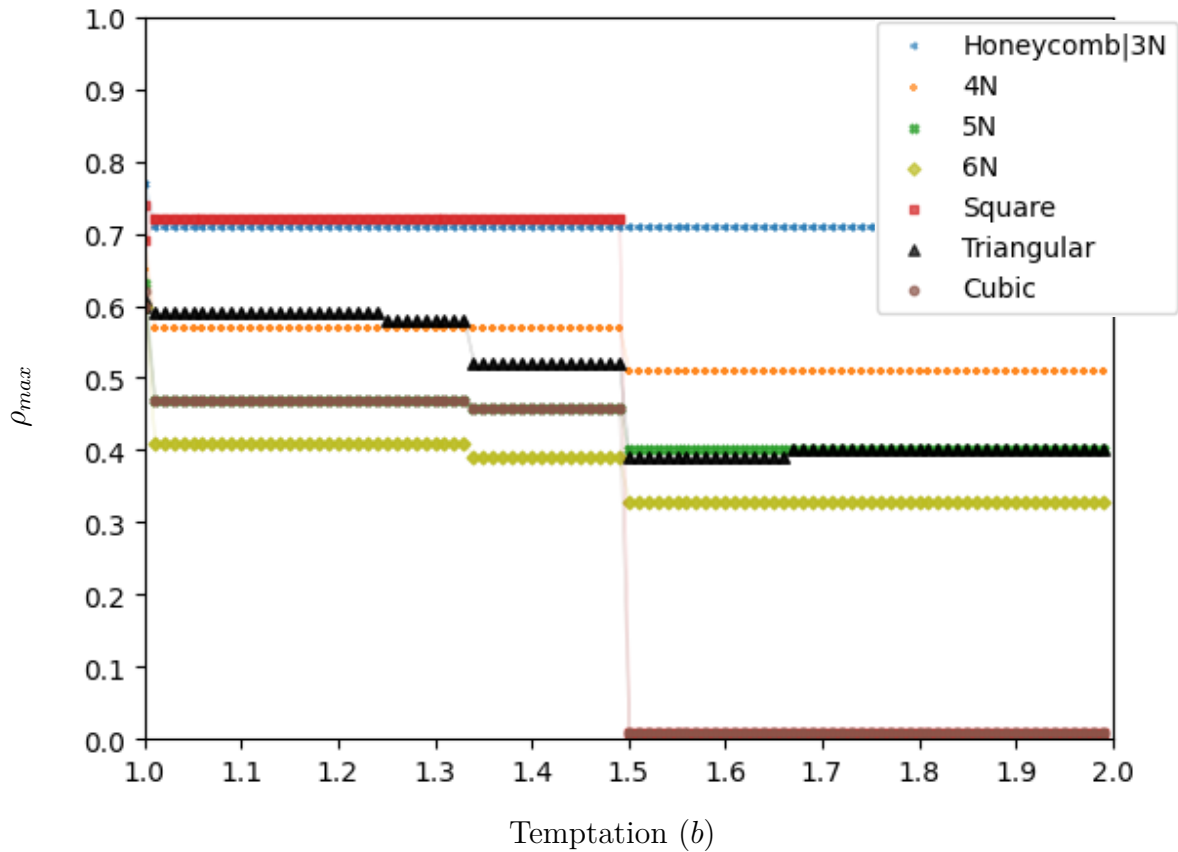


Figure 21 – Different lattice ρ_{max} comparison for Heaviside transition functions.

We display an overview of the site occupancy at which there is a maximum of cooperation (ρ_{max}) for each b and each lattice in Figure 21. We can see an interesting behaviour: for $b < 1.5$, ρ_{max} of the Square lattice is close to the ρ_{max} of the 3N Bethe tree and that of the Cubic lattice is close to the 5N Bethe tree. In these cases, ρ_{max} matches more closely that of a uniform tree with one less neighbour than the one with the same number of neighbours. However, looking at the entire range of parameters in Figure 17a and 20, we can see that the behaviour (such as, width of the peak and b transitions) of the Square and Cubic lattices matches more closely the behaviour 4N and 6N Bethe trees, respectively, only dislocated to higher values of ρ and whole regions of cooperation disappearing (specially for higher b). We can see this for the square by comparing Figure 17a with 20a and 20b, and for the cubic comparing Figure 20e with 20c and 20d.

We present ρ_{max} for the highest b in which the cooperation peak appears (ρ_*) so we can compare to values of the percolation threshold (ρ_{crit}) from the literature in

Lattice	Neighbours	ρ_{crit}	ρ_* (Heaviside)
Honeycomb (3N Bethe)	3	0.69 (0.5) [†]	0.70
Square	4	0.59	0.72
Triangular	6	1/2	0.38 (0.51) [‡]
Cubic	6	0.31	0.46
4N Bethe	4	0.33	0.51 (0.56) [‡]
5N Bethe	5	0.25	0.46
6N Bethe	6	0.20	0.38

Table 6 – Values of ρ_{crit} for different lattices (rounded to within 0.01 variation), obtained from: [Essam \(1980\)](#) for N Bethe $\rho_{crit} = 1/(N-1)$; [Djordjevic, Stanley & Margolina \(1982\)](#) for square and honeycomb; [Sykes & Essam \(1964\)](#) for triangular; [Wang et al. \(2013\)](#) for cubic.

[†] For the 3N Bethe lattice: $\rho_{crit} = 0.5$ and for the honeycomb $\rho_{crit} = 0.69$.

[‡] In the triangular (4N Bethe), the higher peak of cooperators' fraction for lower b ($b < 1.5$) is at $\rho = 0.51$ ($\rho = 0.56$), while the fainter one with higher b ($b > 1.5$) is at $\rho = 0.38$ ($\rho = 0.51$).

Table 6. We can see that for increasing N, the Bethe lattice ρ_* decreases. And, adding more connections in the local topology (as a square or cubic lattice can be compared to 4N and 6N with addition of some connections), the ρ_* also increases. Besides these general observations, we can see that the $\rho_* = 0.7$ for the Honeycomb almost matches $\rho_{crit} \approx 0.69$ of this lattice, but this approximation could be used as well for a 3N Bethe tree, which has a lower $\rho_{crit} = 0.5$. Interestingly, the stronger peak (for $b < 1.5$) for the 4N Bethe lattice ($\rho_* = 0.56$) also falls close to the percolation threshold for the Square lattice ($\rho_* \approx 0.59$). This could be evidence to the peak of cooperation really being due to changes in the local payoff structure. These benefits match coincidentally (or not so, as the local structure is linked to the larger percolation) the percolation threshold. We also think further investigation in MC simulations for the Honeycomb, Triangular and Cubic lattices (as well as possibly studying the behaviour in Bethe trees) is needed, as even in Figure 2 from [Wang, Szolnoki & Perc \(2012a\)](#), it is not clear whether the peaks in cooperation for higher b go to the percolation threshold. And, in the case of the triangular lattice, we can even see it receding to higher ρ for higher b , rather than getting closer to the percolation threshold.

4 Discussion

We began with the idea to develop extended mean-field approximations for different lattices, with the intention to better understand the relation between cooperation and percolation, a problem presented by Wang, Szolnoki & Perc (2012a). Analysing influential papers, like Szabo & Toke (1998) (which uses extended approximations for GT in square lattices) and its referenced papers (DICKMAN, 1988; GUTOWITZ; VICTOR; KNIGHT, 1987; SZABO; SZOLNOKI, 1996), we found the explanations to be poor in clarifying which and how the approximations are built. However, there is a solid mathematical framework for the one dimensional case (GUTOWITZ; VICTOR; KNIGHT, 1987) and trees (non-cyclic graphs) (FANNES; VERBEURE, 1984), but the approximations for two dimensional lattices seemed ambiguous on how to build them for different extended frames, and even how to choose them. It is common to see the use of the pair approximation for the Bethe tree with 4 neighbours as a pair approximation for the square lattice (HAUERT; SZABO, 2005; SZABO; FATH, 2007, p. 207). Even when there is an explanation to the different contributions to the partial equations, it is poorly given and misses one important part: the ΔN counting function, which happens in Hauert & Szabo (2005). Also, since the extended frame is an arbitrary choice, these choices when not properly explained can compromise the reproducibility of the presented results, which is the case in the Szabo & Toke (1998), where the pair approximation used is the Extended Pair approximation, instead of the usual Simple Pair approximation used and explained by the same author in Hauert & Szabo (2005), Szabo & Fath (2007, p. 207).

Considering this, we decided to describe a standard method of generating the approximations through a detailed step-by-step algorithm (section 2.4), based on the ideas in Gutowitz & Victor (1987), we used the core concept of the Bayesian extension process, only we explained it through the concepts of over/underrepresentation of structures. In section 2.5, we exemplified the application of this algorithm to a specific case of a square approximation in a square lattice, so there is a didactic example to be explored. Before this, for purely educational reasons, we introduced a mean-field approximation (section 2.1) and a pair approximation (section 2.2) to simplify the description and exemplification of the concepts used for the creation of the approximation (frames and blocks), which are later formally introduced in section 2.3.1.

To better understand the use of different extended frames and how to choose them, we studied a single system on the square lattice using different central and extended frames. Through comparison with Monte Carlo simulations, we discussed the effects of different extended frames and resumed our findings in the form of a guideline in section 2.7.4. These findings must be validated in other systems, a task for future works. An interesting

case is the Connected Pair approximation which yielded much better predictions than the usually used Simple Pair approximation. We also observed the relevance of the ΔN counting function, since choosing an extended frame inappropriate to the process under consideration can lead to miscomputation in ΔN and a consequent poor performance of the approximation.

We decided to apply the approximations to the diluted lattices in the simplest way, considering holes to be an unchanging-uncopyable state. This particular view raises a question on how much setting the payoff zero for holes may change the system behaviour, but this question is not further pursued. Using the Connected Pair approximation for the square lattice yielded good qualitative results, even fantastically predicting numerically at which ρ the peak of cooperation disappears with increasing temptation b . Further studies showed that these predictions are sensitive to changes in the noise parameter K . This result raises the suspicion that the relation to percolation may come more as a coincidence, at least for the pair approximation, since the boost of cooperation may be related to changes in the local configurations associated with changes in the ω transition functions. We also developed pair approximations for the honeycomb, triangular and cubic lattices (besides analysing the cases for regular trees with less than 6 neighbours). In this analysis, we found the same behaviour as in the square lattice. A further study is needed in MC simulations to check if it presents the same behaviour. Also, further explorations with direct changes to the ω transition tables may present interesting results. We believe that a study of the state evolution in the pair approximations, instead of just the final stable state, through visualization of the three dimensional vector field (similar to what was done in Figure 3, but three dimensional) may collaborate to the understanding of this cooperation boost for certain ρ and b values. Also, for better numerical predictions, increasing the size of the central frame is important, as pointed out by [Xu et al. \(2016\)](#).

We hope this work allows the easy construction of approximations for different systems with its specifics being considered. Further extensions of this work could include innovative dynamics, diffusion/mobility, birth and death process, as well as an analysis of other games and more complicated strategies. Also we hope to see the application of this automated extension process to produce approximations for other kinds of graphs and lattices. Another expansion of this work could be verifying whether the proposed algorithm, as well as the guideline for choosing the extended frame, indeed leads to better approximations.

Bibliography

- AXELROD, R. *The Evolution of Cooperation*. New York, US: Basic Books, 1984. ISBN 0-465-02122-0. Cited in page 3.
- AXELROD, R.; HAMILTON, W. D. The evolution of cooperation. *Science*, American Association for the Advancement of Science, vol. 211, n. 4489, p. 1390–1396, 1981. Available at: <<https://www.jstor.org/stable/1685895>>. Cited in page 3.
- CALHOUN, J. B. Population density and social pathology. *Scientific American*, Scientific American, a division of Nature America, Inc., vol. 206, n. 2, p. 139–149, 1962. ISSN 00368733, 19467087. Available at: <<https://www.jstor.org/stable/24937233>>. Cited in page 5.
- DICKMAN, R. Mean-field theory of the driven diffusive lattice gas. *Phys. Rev. A*, American Physical Society, vol. 38, p. 2588–2593, 1988. Available at: <<https://doi.org/10.1103/PhysRevA.38.2588>>. Cited 2 times in pages 15 and 53.
- DICKMAN, R. Driven lattice gas with repulsive interactions: Mean-field theory. *Phys. Rev. A*, American Physical Society, vol. 41, p. 2192–2195, 1990. Available at: <<https://doi.org/10.1103/PhysRevA.41.2192>>. Cited in page 15.
- DJORDJEVIC, Z. V.; STANLEY, H. E.; MARGOLINA, A. Site percolation threshold for honeycomb and square lattices. *Journal of Physics A: Mathematical and General*, IOP Publishing, vol. 15, n. 8, p. L405–L412, 1982. Available at: <<https://doi.org/10.1088/0305-4470/15/8/006>>. Cited in page 52.
- ESSAM, J. W. Percolation theory. *Reports on Progress in Physics*, IOP Publishing, vol. 43, n. 7, p. 833–912, 1980. Available at: <<https://doi.org/10.1088/0034-4885/43/7/001>>. Cited 2 times in pages 5 and 52.
- FANNES, M.; VERBEURE, A. On solvable models in classical lattice systems. *Communications in Mathematical Physics*, vol. 96, n. 1, p. 115–124, 1984. ISSN 1432-0916. Available at: <<https://doi.org/10.1007/BF01217350>>. Cited in page 53.
- FUKŠ, H. K. Construction of local structure maps for cellular automata. *Journal of Cellular Automata*, vol. 7, 2012. Available at: <<https://arxiv.org/abs/1304.8035v2>>. Cited in page 7.
- GRIMMETT, G.; GRIMMETT, S.; CHERN, S.; ECKMANN, B.; HIRONAKA, H. *Percolation*. Springer, 1999. ISBN 9783540649021. Available at: <<https://www.springer.com/gp/book/9783540649021>>. Cited in page 5.
- GUTOWITZ, H.; VICTOR, J. D. Local structure theory in more than one dimension. *Complex Systems*, vol. 1, p. 57–68, 1987. Available at: <https://www.complex-systems.com/abstracts/v01_i01_a05/>. Cited 7 times in pages v, vii, 7, 15, 16, 20, and 53.
- GUTOWITZ, H.; VICTOR, J. D. Local structure theory: Calculation on hexagonal arrays, interaction of rule and lattice. *Journal of Statistical Physics*, vol. 54, 1994. Available at: <<https://www.doi.org/10.1007/BF01023491>>. Cited in page 15.

GUTOWITZ, H.; VICTOR, J. D.; KNIGHT, B. W. Local structure theory for cellular automata. *Physica D: Nonlinear Phenomena*, p. 18–48, 1987. Available at: [https://doi.org/10.1016/0167-2789\(87\)90120-5](https://doi.org/10.1016/0167-2789(87)90120-5). Cited 3 times in pages 15, 19, and 53.

HAUERT, C.; SZABO, G. Game theory and physics. *American Journal of Physics*, vol. 73, n. 5, p. 405–414, 2005. Available at: <https://doi.org/10.1119/1.1848514>. Cited 3 times in pages 9, 35, and 53.

HIEBELER, D. Stochastic spatial models: From simulations to mean field and local structure approximations. *Journal of Theoretical Biology*, vol. 187, n. 3, p. 307 – 319, 1997. ISSN 0022-5193. Available at: <https://doi.org/10.1006/jtbi.1997.0422>. Cited in page 15.

LEIVAS, F. *Dinâmicas estocásticas em teoria de jogos : percolação, cooperação e seus limites*. Dissertação (Mestrado) — Instituto de Física - UFRGS, Porto Alegre, BR-RS, 2018. Available at: <http://hdl.handle.net/10183/183168>. Cited in page 41.

MALTHUS, T. R. *An essay on the principle of population: Or, a view of its past and present effects on human happiness, with an inquiry into our prospects respecting the future removal or mitigation of the evils which it occasions*. London, UK: Reeves and Turner, 1878. Cited in page 5.

MAYNARD, J. S. *Evolution and the Theory of Games*. Cambridge, UK: Cambridge University Press, 1982. ISBN 9780521246736. Available at: <https://doi.org/10.1017/CBO9780511806292>. Cited 2 times in pages 3 and 4.

MELONI, S.; BUSCARINO, A.; FORTUNA, L.; FRASCA, M.; GÓMEZ-GARDEÑES, J.; LATORA, V.; MORENO, Y. Effects of mobility in a population of prisoner's dilemma players. *Phys. Rev. E*, vol. 79, p. 067101, 2009. Available at: <https://doi.org/10.1103/PhysRevE.79.067101>. Cited in page 5.

Merriam-Webster Online Dictionary. *Game*. 2021. [Online; accessed 28 Jan. 2021]. Available at: <https://www.merriam-webster.com/dictionary/game>. Cited in page 1.

NASH, J. F. Equilibrium points in n-person games. *Proceedings of the National Academy of Sciences*, National Academy of Sciences, vol. 36, n. 1, p. 48–49, 1950. Available at: <https://doi.org/10.1073/pnas.36.1.48>. Cited in page 1.

NOWAK, M.; MAY, R. Evolutionary games and spatial chaos. *Nature*, vol. 359, p. 826–829, 1992. Available at: <https://doi.org/10.1038/359826a0>. Cited 3 times in pages v, vii, and 4.

NOWAK, M. A. Five rules for the evolution of cooperation. *Science*, American Association for the Advancement of Science, vol. 314, n. 5805, p. 1560–1563, 2006. ISSN 0036-8075. Available at: <https://doi.org/10.1126/science.1133755>. Cited in page 4.

PERC, M.; SZOLNOKI, A. Social diversity and promotion of cooperation in the spatial prisoners dilemma game. *Phys. Rev. E*, American Physical Society (APS), vol. 77, n. 1, 2008. ISSN 1550-2376. Available at: <https://doi.org/10.1103/PhysRevE.77.011904>. Cited in page 5.

- POUNDSTONE, W. *Prisoner's Dilemma / John Von Neumann, game theory and the puzzle of the bomb*. New York, US: Anchor, 1993. ISBN 978-0385415804. Cited 2 times in pages 2 and 3.
- SICARDI, E. A.; FORT, H.; VAINSTEIN, M. H.; ARENZON, J. J. Random mobility and spatial structure often enhance cooperation. *Journal of Theoretical Biology*, vol. 256, n. 2, p. 240 – 246, 2009. ISSN 0022-5193. Available at: <<https://doi.org/10.1016/j.jtbi.2008.09.022>>. Cited in page 5.
- SYKES, M. F.; ESSAM, J. W. Exact critical percolation probabilities for site and bond problems in two dimensions. *Journal of Mathematical Physics*, vol. 5, n. 8, p. 1117–1127, 1964. Available at: <<https://doi.org/10.1063/1.1704215>>. Cited in page 52.
- SZABO, G.; FATH, G. Evolutionary games on graphs. *Physics Reports*, vol. 446, n. 4, p. 97 – 216, 2007. ISSN 0370-1573. Available at: <<https://doi.org/10.1016/j.physrep.2007.04.004>>. Cited 9 times in pages 1, 3, 4, 14, 28, 35, 44, 53, and 73.
- SZABO, G.; SZOLNOKI, A. Generalized mean-field study of a driven lattice gas. *Phys. Rev. E*, American Physical Society, vol. 53, p. 2196–2199, 1996. Available at: <<https://doi.org/10.1103/PhysRevE.53.2196>>. Cited in page 53.
- SZABO, G.; TOKE, C. Evolutionary prisoner's dilemma game on a square lattice. *Phys. Rev. E*, American Physical Society, vol. 58, p. 69–73, 1998. Available at: <<https://doi.org/10.1103/PhysRevE.58.69>>. Cited 5 times in pages 7, 15, 30, 35, and 53.
- SZABO, G.; VUKOV, J.; SZOLNOKI, A. Phase diagrams for an evolutionary prisoner's dilemma game on two-dimensional lattices. *Phys. Rev. E*, American Physical Society, vol. 72, p. 047107, 2005. Available at: <<https://doi.org/10.1103/PhysRevE.72.047107>>. Cited in page 4.
- SZOLNOKI, A.; PERC, M.; DANKU, Z. Towards effective payoffs in the prisoners dilemma game on scale-free networks. *Physica A: Statistical Mechanics and its Applications*, vol. 387, n. 8, p. 2075 – 2082, 2008. ISSN 0378-4371. Available at: <<https://doi.org/10.1016/j.physa.2007.11.021>>. Cited 2 times in pages 4 and 43.
- VAINSTEIN, M. H.; ARENZON, J. J. Disordered environments in spatial games. *Phys. Rev. E*, American Physical Society, vol. 64, p. 051905, 2001. Available at: <<https://doi.org/10.1103/PhysRevE.64.051905>>. Cited 4 times in pages v, vii, 5, and 41.
- VAINSTEIN, M. H.; T.C. SILVA, A.; ARENZON, J. J. Does mobility decrease cooperation? *Journal of Theoretical Biology*, vol. 244, n. 4, p. 722 – 728, 2007. ISSN 0022-5193. Available at: <<https://doi.org/10.1016/j.jtbi.2006.09.012>>. Cited in page 5.
- Von Neumann, J.; MORGENSTERN, O. *Theory of games and economic behavior*. Princeton, US: Princeton University Press, 1944. ISBN 978-0691130613. Cited in page 1.
- WANG, J.; ZHOU, Z.; ZHANG, W.; GARONI, T. M.; DENG, Y. Bond and site percolation in three dimensions. *Phys. Rev. E*, American Physical Society, vol. 87, p. 052107, 2013. Available at: <<https://doi.org/10.1103/PhysRevE.87.052107>>. Cited in page 52.

WANG, Z.; SZOLNOKI, A.; PERC, M. If players are sparse social dilemmas are too: Importance of percolation for evolution of cooperation. *Scientific Reports*, vol. 2, n. 369, p. 2045–2322, 2012. Available at: <<https://doi.org/10.1038/srep00369>>. Cited 10 times in pages v, vii, 5, 41, 43, 44, 45, 52, 53, and 74.

WANG, Z.; SZOLNOKI, A.; PERC, M. Percolation threshold determines the optimal population density for public cooperation. *Phys. Rev. E*, American Physical Society, vol. 85, p. 037101, 2012. Available at: <<https://doi.org/10.1103/PhysRevE.85.037101>>. Cited in page 5.

WU, Z.-X.; GUAN, J.-Y.; XU, X.-J.; WANG, Y.-H. Evolutionary prisoner's dilemma game on Barabási-Albert scale-free networks. *Physica A: Statistical Mechanics and its Applications*, vol. 379, n. 2, p. 672 – 680, 2007. ISSN 0378-4371. Available at: <<https://doi.org/10.1016/j.physa.2007.02.085>>. Cited in page 4.

XU, C.; ZHANG, W.; DU, P.; CHOI, C. W.; HUI, P. M. Understanding cooperative behavior in structurally disordered populations. *Eur. Phys. J. B*, vol. 89, n. 6, p. 152, 2016. Available at: <<https://doi.org/10.1140/epjb/e2016-60826-y>>. Cited 4 times in pages 41, 42, 43, and 54.

Appendices

APPENDIX A – Is the Weak PD with Self-Interaction a Snowdrift game?

It is common in eGT to include self-interaction, that is, adding an interaction where the player plays one time with itself. This grants a great benefit to cooperators in a weak PD, since they receive $R = 1$ for this auto-interaction and defectors receive $P = 0$. We could, of course, include this in the payoff matrix instead of counting it as an auto-interaction, we can even claim that this is the expected way a rational player would compute the payoff matrix. Provided that the player plays with n neighbours (in the square lattice $n = 4$), a cooperator gets $1/n$ more in each interaction (independent if it is against a cooperator or a defector) and a defector gets no benefit. Therefore, we can rewrite the Payoff Table 1b as:

		Player Y	
		C	D
Player X	C	$1 + 1/n$	$1/n$ / b
	D	b / $1/n$	0

(a) Payoff in the weak Prisoner's Dilemma game with self-interaction.

		Player Y	
		C	D
Player X	C	1	$bn/(n+1)$ / $1/(n+1)$
	D	$bn/(n+1)$ / $1/(n+1)$	0

(b) We perform a rescaling of the payoff table to maintain $R = 1$, $P = 0$ by dividing all values by $1 + 1/n = (n + 1)/n$.

Table 7 – Two versions of the payoff matrix for the weak Prisoner's Dilemma game with self-interaction. The second payoff matrix is rescaled to maintain $R = 1$, $P = 0$.

We can clearly see, in Payoff Table 7a, that the payoff for cooperating with a defector ($1/n$) is higher than defecting with a defector (0). This means that the $P \geq S$ condition is not met changing this game into a Snowdrift (also named, Hawk-Dove) in the case where $b > 1 + 1/n$. It certainly follows the condition $T > R > S > P$, meaning it can be read as a Snowdrift game. Looking at Payoff Table 7b, we find that the values will match the common parametrization for Hawk-Dove $R = 1$, $T = 1 + r$, $S = 1 - r$, $P = 0$, only at $b = 2 + 1/n$ ($r = n/(n + 1)$) which normally is not an explored value, since the limitations for a weak PD not becoming an anti-coordination game is $b < 2$.

APPENDIX B – Approximations for the square lattice

Here we will detail the approximations used in section 2.7, by defining for each one its extended frame, the equation for its block approximation probability function and presenting a visual representation of this approximation.

The extended frames will be defined by selecting different parts of the graph in Figure 22. The graph shows 20 named sites that form a part of a square lattice.

More information on the approximations are in Table 8 for the pair, Table 9 for the square and Table 10 for the cross approximations. In the following sections, we will write the equation for its block approximation probability function.

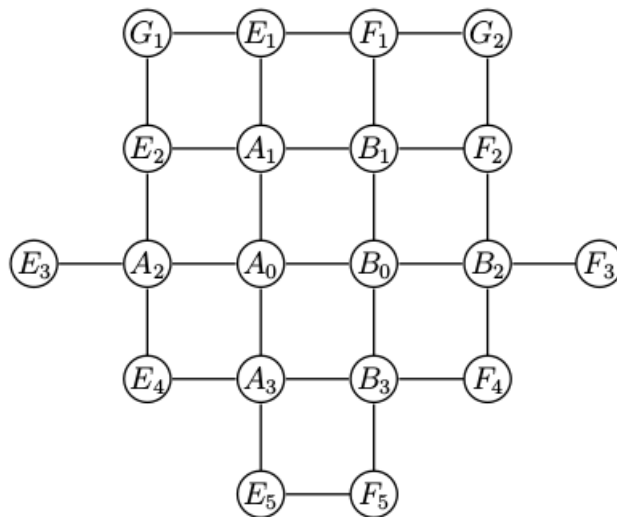


Figure 22 – A graph representing part of a square lattice. We will select different parts as the extended frame to build different approximations.

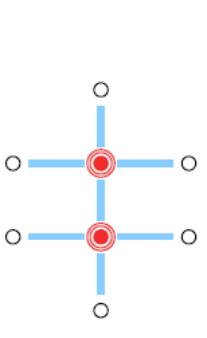
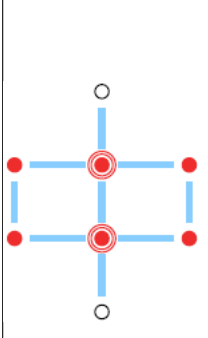
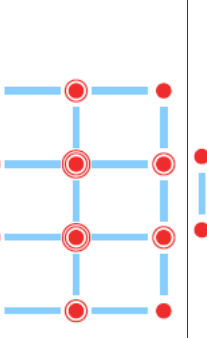
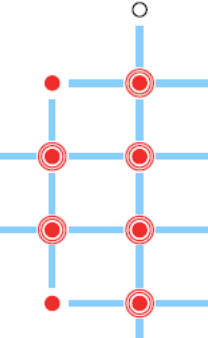
Approximation	Central Frame	Extended Frame	Visual Representation	Equation	Notes
Simple Pair	A_0, B_0	$A_0, B_0, A_1, A_2, A_3, B_1, B_2, B_3$		(B.1)	This is the most commonly used when referring to pair approximation. Correlations between A_1, B_1 and between A_3, B_3 are not included.
Connected Pair	A_0, B_0	$A_0, B_0, A_1, A_2, A_3, B_1, B_2, B_3$		(B.2)	This is the one that performed best among the pair approximations, according to results in Section 2.7.1.
Extended Pair	A_0, B_0	$A_0, B_0, A_1, A_2, A_3, B_1, B_2, B_3, E_2, E_4, F_2, F_4$		(B.3)	
Second Neighbours Pair	A_0, B_0	$A_0, B_0, A_1, A_2, A_3, B_1, B_2, B_3, E_1, E_2, E_3, E_4, F_1, F_2, F_3, F_4$		(B.4)	This could be used in a game where the players plays with its first and second neighbours.

Table 8 – Pair approximations for the square lattice, the extended frames can be seen as parts of the lattice in Figure 22.

Approximation	Central Frame	Extended Frame	Visual Representation	Equation	Notes
Reduced Square	A_0, B_0, A_1, B_1	$A_0, B_0, A_1, A_2, A_3, B_1, B_2, B_3, E_1, E_2, F_1, F_2$		(B.5)	This extended frame miscounts changes in ΔN function.
4x4 Square	A_0, B_0, A_1, B_1	$A_0, B_0, A_1, A_2, A_3, B_1, B_2, B_3, E_1, E_2, E_4, F_1, F_2, F_4, G_1, G_2$		(B.7)	
3x4 Square	A_0, B_0, A_1, B_1	$A_0, B_0, A_1, A_2, A_3, B_1, B_2, B_3, E_2, E_4, F_2, F_4$		(B.6)	We can only consider changes in A_0 and B_0 .
Mixed Square	A_0, B_0, A_1, B_1	$A_0, B_0, A_1, A_2, A_3, B_1, B_2, B_3, E_2, E_4$		(B.8)	We can only consider changes in A_0 . This approximation could be improved by using an L-shaped frame.

Table 9 – Square (4-point) approximations for the square lattice, the extended frames can be seen as parts of the lattice in Figure 22.

Approximation	Central Frame	Extended Frame	Visual Representation	Equation	Notes
Minimal Cross	A_0, B_0, A_1, A_2, A_3	$A_0, B_0, A_1, A_2, A_3, B_1, B_2, B_3, E_1, E_2, E_3, E_4, E_5$		(B.9)	We can only consider changes in the state of A_0 . For the ΔN wrong counting example, we considered changes in all of the central frame.
Double Cross	A_0, B_0, A_1, A_2, A_3	$A_0, B_0, A_1, A_2, A_3, B_1, B_2, B_3, E_1, E_2, E_3, E_4, F_1, F_2, F_3, F_4, F_5$		(B.10)	We can consider changes in the state of A_0 and B_0

Table 10 – Cross (5-point) approximations for the square lattice, the extended frames can be seen as parts of the lattice in Figure 22. These approximations could be made better by using L-shape frames and “diagonal neighbour” frames, but we did not test with those.

B.1 Pair approximations

The four different pair approximations we used are defined in Table 8, and their block probabilities are defined in the following equations.

For the simple pair approximation:

$$P_{simple} = \frac{P_-(A_0, B_0)}{P_o^3(A_0) P_o^3(B_0)} \prod_{i=1}^3 [P_-(A_0, A_i) P_-(B_0, B_i)] \quad (\text{B.1})$$

For the connected pair approximation:

$$P_{conn} = P_{simple} \times \frac{P_-(A_1, B_1)}{P_o(A_1) P_o(B_1)} \frac{P_-(A_3, B_3)}{P_o(A_3) P_o(B_3)} \quad (\text{B.2})$$

For the extended pair approximation:

$$P_{ext} = P_{conn} \times \frac{P_-(E_2, A_1) P_-(E_2, A_2)}{P_o(E_2) P_o(A_1) P_o(A_2)} \frac{P_-(E_4, A_3) P_-(E_4, A_2)}{P_o(E_4) P_o(A_3) P_o(A_2)} \times \\ \times \frac{P_-(F_2, B_1) P_-(F_2, B_2)}{P_o(F_2) P_o(B_1) P_o(B_2)} \frac{P_-(F_4, B_3) P_-(F_4, B_2)}{P_o(F_4) P_o(B_3) P_o(B_2)} \quad (\text{B.3})$$

For the second neighbours pair approximation:

$$P_{2nd} = P_{ext} \times \frac{P_-(A_2, E_3)}{P_o(A_2)} \frac{P_-(B_2, F_3)}{P_o(B_2)} \frac{P_-(A_1, E_1)}{P_o(A_1)} \frac{P_-(B_1, F_1)}{P_o(B_1)} \frac{P_-(E_1, F_1)}{P_o(E_1) P_o(F_1)} \times \\ \times \frac{P_-(A_3, E_5)}{P_o(A_3)} \frac{P_-(B_3, F_5)}{P_o(B_3)} \frac{P_-(E_5, F_5)}{P_o(E_5) P_o(F_5)} \quad (\text{B.4})$$

B.2 Square approximations

The four different square approximations we used are defined in Table 9; their block probabilities are defined in the following equations.

For the reduced square approximation (the one that leads to miscounting of the ΔN function):

$$P_{red} = \frac{P_{\square}(A_0, B_0, A_1, B_1) P_{\square}(A_0, B_0, A_3, B_3) P_{\square}(A_0, A_1, E_2, A_2)}{P_-(A_0, B_0) P_-(A_0, A_1)} \times \\ \times \frac{P_{\square}(B_0, B_1, F_2, B_2) P_{\square}(A_1, B_1, F_1, E_1)}{P_-(B_0, B_1) P_-(B_1, A_1)} \quad (\text{B.5})$$

For the 3×4 square approximation:

$$P_{3 \times 4} = \frac{P_{\square}(A_0, B_0, A_1, B_1) P_{\square}(A_0, B_0, A_3, B_3) P_{\square}(A_0, A_1, E_2, A_2) P_{\square}(A_0, A_3, E_4, A_2)}{P_-(A_0, B_0) P_-(A_0, A_1) P_-(A_0, A_2) P_-(A_0, A_3)} \times \\ \times \frac{P_{\square}(B_0, B_1, F_2, B_2) P_{\square}(B_0, B_3, F_4, B_2)}{P_-(B_0, B_1) P_-(B_0, B_2) P_-(B_0, B_3)} P_o(A_0) P_o(B_0) \quad (\text{B.6})$$

For the 4×4 square approximation:

$$P_{4 \times 4} = P_{3 \times 4} \times \frac{P_{\square}(A_1, E_1, G_1, E_2)P_{\square}(A_1, E_1, F_1, B_2)P_{\square}(B_1, F_1, G_2, F_2)}{P_{-}(A_1, E_2)P_{-}(A_1, B_1)P_{-}(A_1, F_2)P_{-}(A_1, E_1)P_{-}(B_1, F_1)} P_{\circ}(A_1)P_{\circ}(B_1) \quad (\text{B.7})$$

For the mixed square approximation:

$$P_{mix} = \frac{P_{\square}(A_0, B_0, A_1, B_1)P_{\square}(A_0, B_0, A_3, B_3)P_{\square}(A_0, A_1, E_2, A_2)P_{\square}(A_0, A_3, E_4, A_2)}{P_{-}(A_0, B_0)P_{-}(A_0, A_1)P_{-}(A_0, A_2)P_{-}(A_0, A_3)} \times \\ \times P_{-}(B_0, A_2) \frac{P_{\circ}(A_0)}{P_{\circ}(B_0)} \quad (\text{B.8})$$

B.3 Cross Approximations

The two different cross approximations we used are defined in Table 10; their block probabilities are defined in the following equations.

For the minimal cross approximation:

$$P_{cross} = \frac{P_{+}(A_0, A_1, A_2, A_3, B_0)P_{+}(A_1, E_1, E_2, A_0, B_1)P_{+}(A_2, E_2, E_3, E_4, A_0)}{P_{-}(A_0, B_0)P_{-}(A_0, A_1)P_{-}(A_0, A_2)P_{-}(A_0, A_3)} \times \\ \times \frac{P_{+}(A_3, A_0, E_4, E_5, B_3)P_{+}(B_0, B_1, A_0, B_3, B_2)}{P_{\circ}(E_2)P_{\circ}(E_4)P_{\circ}(B_2)P_{\circ}(B_4)} \quad (\text{B.9})$$

For the double cross approximation:

$$P_{double} = P_{cross}P_{\circ}(B_2)P_{\circ}(B_4) \times \frac{P_{+}(B_1, F_1, A_1, B_0, F_2)P_{+}(B_2, F_2, B_0, F_4, F_3)}{P_{-}(A_1, B_1)P_{-}(A_3, B_3)P_{-}(B_0, B_1)P_{-}(B_0, B_2)P_{-}(B_0, B_3)} \times \\ \times \frac{P_{+}(B_3, B_0, A_3, F_5, F_4)P_{-}(E_1, F_1)P_{-}(E_5, F_5)}{P_{\circ}(E_1)P_{\circ}(E_5)P_{\circ}(F_1)P_{\circ}(F_5)P_{\circ}(F_2)P_{\circ}(F_4)} \quad (\text{B.10})$$

APPENDIX C – Pair Approximations for Diverse Lattices

We present in this appendix the pair approximations used for lattices besides the square lattice. We define the extended frames used in each case and present the equation for the block probability for the extended frame. For the Honeycomb, Cubic and Triangular lattices, we also present the graphed form of the extended frame and the visual representation of its pair approximation.

C.1 Pair Approximation for the N Bethe trees

For a Bethe lattice with N neighbours, we consider a central pair formed by players A_0 and B_0 , naming the first neighbours of A as $A_1 \cdots A_{N-1}$ and the first neighbours of B as $B_1 \cdots B_{N-1}$. The pair approximation for the extended frame $j = A_0 B_0 A_1 \cdots A_{N-1} B_1 \cdots B_{N-1}$ ($2N$ sites) can be written as:

$$P_{N,Bethe}(j) = P_-(A_0B_0) \prod_{i=1}^{N-1} \frac{P_-(A_0A_i)P_-(B_0B_i)}{P(A_0)P(B_0)} \quad (C.1)$$

$$= \frac{P_-(A_0B_0)}{[P(A_0)P(B_0)]^{N-1}} \prod_{i=1}^{N-1} P_-(A_0A_i)P_-(B_0B_i) \quad (C.2)$$

For $N = 4$, this approximation is equivalent to the Simple Pair approximation for the square lattice, explained in Appendix B, equation B.1. Equivalently, we could use $N = 6$ for an approximation for the Cubic lattice, disregarding the relations existent among their first neighbours.

C.2 Pair Approximation for the Honeycomb Lattice

For the honeycomb lattice, since no cyclic structure can be seen analysing just the pair and its first neighbours, we use the approximation for the Bethe tree with $N = 3$, for a state $j = A_0B_0A_1A_2B_1B_2$ (the graph formed by them is represented in Figure 23a):

$$P_{honeycomb}(j) = \frac{P_-(A_0B_0)}{[P(A_0)P(B_0)]^2} P_-(A_0A_1)P_-(A_0A_2)P_-(B_0B_1)P_-(B_0B_2). \quad (C.3)$$

The visual representation of this pair approximation for the honeycomb lattice is presented in Figure 23b.

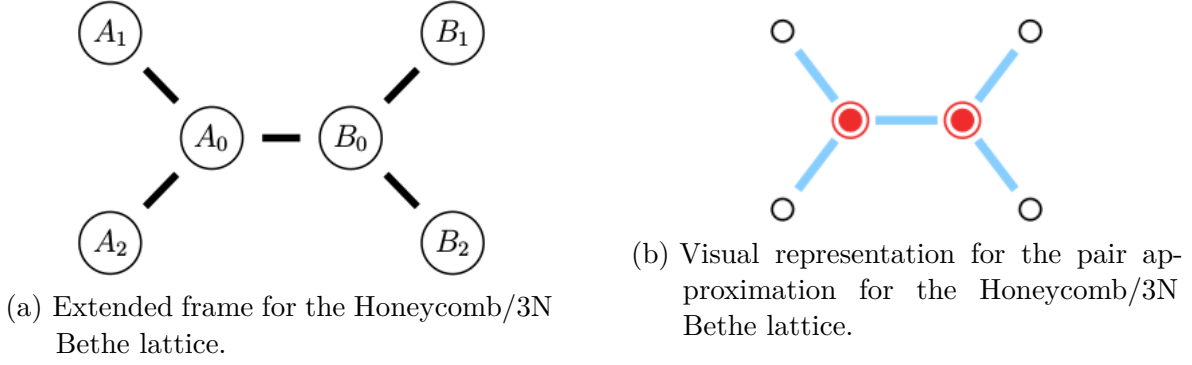


Figure 23 – Extended Frame and visual representation for its pair approximation used for the Honeycomb lattice/3N Bethe tree.

C.3 Pair Approximation for the Cubic Lattice

We present the extended frame (the central pair and its first neighbours, totaling 12-sites) for the pair approximation for the cubic lattice in Figure 24a. The block pair probability for the state $j = A_0 B_0 A_1 \cdots A_5 B_1 \cdots B_5$ is :

$$P_{cubic}(j) = P_{6,Bethe}(j) \times \prod_{i=1,3,4,5} \frac{P_-(A_i B_i)}{P(A_i)P(B_i)} \quad (C.4)$$

$$= P_{conn}(A_0 B_0 A_1 A_2 A_3 B_1 B_2 B_3) \times \left[\prod_{i=4,5} \frac{P_-(A_0 A_i) P_-(B_0 B_i) P_-(A_i B_i)}{P(A_0) P(B_0) P(A_i) P(B_i)} \right], \quad (C.5)$$

where, in equation (C.4), we take in consideration a 6N Bethe lattice and multiply by the other connections the neighbours have. In equation (C.5), we consider the two dimensional square lattice case and extend adding the sites $A_4 A_5 B_4 B_5$ to form the approximation for the cubic lattice. Both are equivalent. They could be easily generalized to hypercubes of higher dimmensions, specially equation (C.4). We present the pair approximation for the cubic lattice in visual form in Figure 24b.

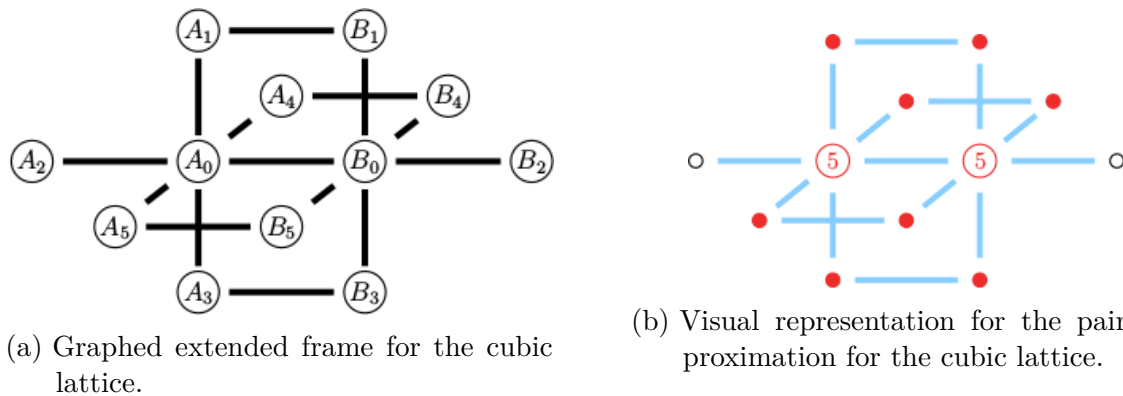


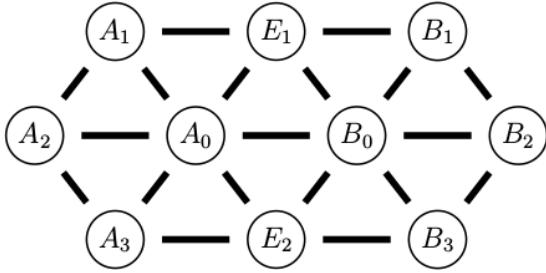
Figure 24 – Extended Frame and visual representation for its pair approximation used for the cubic lattice.

C.4 Pair Approximation for the Triangular Lattice

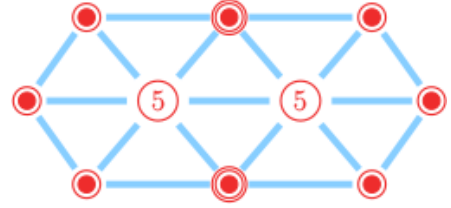
For the triangular lattice, we consider the central pair and its first neighbours, totaling 10 sites, as represented in graph form in Figure 25a. The block pair probability for the state $j = A_0 B_0 E_1 E_2 A_1 A_2 A_3 B_1 B_2 B_3$ is:

$$P_{triang}(j) = P_-(A_0 B_0) \left[\prod_{i=1,2,3} \frac{P_-(A_0 A_i) P_-(B_0 B_i)}{P(A_0) P(B_0)} \right] \times \left[\prod_{i=1,2} \frac{P_-(A_0 E_i) P_-(B_0 E_i)}{P(A_0) P(B_0) P(E_i)} \right] \left[\prod_{i=1}^8 \frac{P_-(K_i K_{i+1})}{P(K_i) P(K_{i+1})} \right], \quad (\text{C.6})$$

where we define that $K_i = [A_1, A_2, A_3, E_2, B_3, B_2, B_1, E_1, A_1]$ (it's a list of the neighbors of the central pair in the anti-clockwise order) to shorten the equation. The visual representation of the pair approximation for the triangular lattice in equation (C.6) is presented in Figure 25b.



(a) Graphed extended frame for the triangular lattice.



(b) Visual representation for the pair approximation for the triangular lattice.

Figure 25 – Extended Frame and visual representation for its pair approximation used for the triangular lattice.

APPENDIX D – Transition function ω

Throughout this work we will use different functions for the transition function ω . These represent chances for the given process to happen (in our case, invasion). We will be using functions based on the payoff difference between two players ΔPay . We will use three different ω functions which assign different probabilities for each ΔPay : Heaviside; Replicator; Fermi (family of functions with parameter K). All of them are non-decreasing functions of ΔPay , that is, $\frac{d\omega}{d\Delta Pay} \geq 0$, which means that a player with a higher payoff has a greater chance of being copied than one with a smaller payoff.

The Heaviside function is an interesting case, where, when comparing a pair, if the payoff of the player is higher than the neighbour's, it is certainly copied (probability one). If it is lower, it will not be copied (probability zero). The definition of Heaviside we used is:

$$\Theta(\Delta Pay) = \begin{cases} 1 & \text{if } \Delta Pay > 0 \\ 0 & \text{if } \Delta Pay \leq 0 \end{cases} . \quad (\text{D.1})$$

The results may change a little for some specific values of b if we define for $\Delta Pay = 0 \Rightarrow \Theta(\Delta Pay) = 0.5$. We did not investigate these cases.

The replicator function comes from some early models in Biology (SZABO; FATH, 2007, p. 118), where the chance of being copied increases linearly with increasing payoff difference, with the condition that the chance of being copied if the payoff difference is negative is null. The definition of the Replicator transition we used is:

$$\omega_{REP}(\Delta Pay) = \begin{cases} \frac{\Delta Pay}{\max(\Delta Pay)} & \text{if } \Delta Pay > 0 \\ 0 & \text{if } \Delta Pay \leq 0 \end{cases} , \quad (\text{D.2})$$

where $\max(\Delta Pay)$ is the maximum payoff difference possible, normalizing this case to probability one. It is interesting that we do not need this normalization $N = 1/\max(\Delta Pay)$ in the approximations as it can be incorporated into the Δt . The same can be argued for MC simulations when we try to use a normalization $N < 1/\max(\Delta Pay)$. For example, if we normalize by $N = 0.5/\max(\Delta Pay)$, we know the system will take double the time, therefore the evolution just needs a rescale in the time to be corresponding.

The Fermi family of functions is defined by a noise K parameter ($K > 0$). It is interesting because we will not have null probabilities of being copied for $\Delta Pay \leq 0$. Allowing players with a smaller payoff to be copied is sometimes referred to as *irrationality*. This property frees some points in the lattice that would be frozen (WANG; SZOLNOKI;

PERC, 2012a). The definition of the Fermi with noise K we used is:

$$\omega_{Fermi}(\Delta Pay) = \frac{1}{1 + e^{-\Delta Pay/K}} . \quad (D.3)$$

Besides being a smooth, continuous function, the Fermi family has the nice property that $\omega_{Fermi}(x) = 1 - \omega_{Fermi}(-x)$. This results that the chance of A invading B is complimentary of the chance of B invading A .

Also, when $K \rightarrow 0$, this function tends to a Heaviside function (with $\Delta Pay = 0 \Rightarrow \Theta(\Delta Pay) = 0.5$) and for $K \rightarrow \infty$, $\omega_{Fermi}(x) = 1/2 \forall x$. This results that, with increasing K parameter, the chances of being copied become more random, introducing a certain noise for the probability of the process happening.